



UNIVERSITY OF GRAZ

BACHELOR THESIS

The ingredients for the π -meson form factor in an Interaction model

Iulian Grozav

supervised by
Univ.-Prof. Dr.rer.nat. Reinhard ALKOEFER

Department of Physics

July 1, 2024

Contents

1	Introduction	3
2	An introduction to QCD	5
2.1	Historic Overview of the Emergence of QCD	5
2.2	QCD Lagrangian	9
2.3	Gauge fixing	10
2.4	Generating DSE for 1PI correlation functions	11
3	Quark DSE	15
4	Pion BSE	18
5	Electromagnetic coupling of quarks	22
5.1	General remarks	22
5.2	Quark-Photon vertex	23
6	Numerical Result	26
7	Summary	32
	Acknowledgement	33
	Appendix A Conventions	34
A.1	Euclidean field theory	34
A.2	Integration over Hyperspherical coordinates	35
	Appendix B QCD Feynman rules	37
B.1	Renormalized QCD Feynman rules	37
B.1.1	Quark Propagator	37
B.1.2	Gluon Propagator	38
B.1.3	Quark-Gluon vertex	38
	Appendix C Truncation scheme	40
C.1	Rainbow-ladder truncation	40
C.2	Maris-Tandy model for the effective interaction	40
	Appendix D Further information to the Quark DSE	42
D.1	Color structure of the quark DSE	42
D.2	Dirac structure of the quark DSE	42
D.3	Analytical angular integration	44

D.4	Explicit expressions for the self energy dressing functions	44
Appendix E	Further information to the Pion BSE	45
E.1	Dirac structure of the pion BSE	45
Appendix F	Further information to the quark-photon vertex	48
F.1	Dirac structure of the quark-photon vertex	48
Bibliography		54

Chapter 1

Introduction

In recent years, there has been a great deal of activity in the field of form factor calculations for hadrons. Form factors encode the momentum-dependent interaction of hadrons with photons. They are a crucial quantity since they can be experimentally probed by scattering leptons off hadrons or scattering hadrons on other hadrons. A fundamental breakthrough was the discovery of Robert Hofstadter in the mid-1960s that the proton and neutron are not point-like elementary particles, but have internal structure. This was described in detail in Hofstadter's Nobel Prize-winning work, cited here as reference [1]. Subsequently, in 1967, a series of experiments concerning deep inelastic scattering of electrons onto protons at MIT-SLAC was conducted, which provided evidence that the internal structure of the proton consists of quarks and gluons [2]. This new postulated particle, the quark, is confined in hadrons and is described in the strong interaction, which is described by a quantum field theory called Quantum Chromodynamics (QCD). Of particular significance are the three pions π , π^\pm . Their unique status arises from their role as Goldstone bosons related to chiral symmetry and its dynamical breaking. The electromagnetic form factor calculation for the pion was achieved, for example, in 1999 by P. Maris and P. Tandy [3]; however, it was solely for spacelike momenta. In 2021, Á. López, H. Alepuz and R. Alkofer made a significant advance in this field by calculating the electromagnetic form factor of the pion at timelike momenta [4]. The objective of this thesis is to provide the essential building blocks required to execute the calculation of electromagnetic form factors for pions in a framework based on functional methods consisting of Bethe-Salpeter equations (BSE) and Dyson-Schwinger equations (DSE). These ingredients include the fully renormalized quark propagator $S(p)$, the Bethe-Salpeter amplitude (BSA) of the pion $\Gamma(p)$ and the quark-photon vertex $\Gamma_{qp}^\mu(p)$.

The framework of functional methods employed here allows us to consider the fully renormalized quark-gluon vertex. However, the numerical costs involved make this approach impractical, and thus a model is employed. In implementing a model, certain criteria must be met. One such criterion is that global symmetries are not violated. For instance, in the case of chiral symmetry and dynamical symmetry breaking, leading to massless pions in the chiral limit, it is essential that these symmetries must be maintained to accurately study the hadronic properties of the pion itself. Conversely, it is essential that charge conservation must not be violated by the model. This is particularly important when handling electromagnetic processes, as is the case here. Any violation of this principle would be an unacceptable approach. The chosen quark-antiquark interaction model, the Rainbow-Ladder truncation, is in accordance with our criteria and consists of a gluon

exchange between the quark and the antiquark.

This thesis begins with a historical overview of the emergence of QCD and a concise derivation of the master equation that generates Dyson-Schwinger equations, as presented in chapter 2. It then proceeds to provide a mathematical description of the aforementioned ingredients in chapters 3, 4, 5, which include the technical tricks in the Appendix. The numerical results are presented in chapter 6, after which the thesis concludes with a summary in chapter 7.

Chapter 2

An introduction to QCD

Since this thesis is based on the formalism of Quantum Chromodynamics (QCD), I want to dedicate this chapter to a concise historical development of QCD, in order to appreciate this theory of the strong force. A very detailed development can be called up from [5].

2.1 Historic Overview of the Emergence of QCD

The birthstone of the strong interaction can be viewed as the discovery of the neutron in 1932 by J. Chadwick [6]. It supports the concept that nuclei consist of protons and neutrons, held together by a powerful force that surpasses electromagnetic repulsion. Due to the similarity of the mass of protons and neutrons, Heisenberg introduced the *Isospin*¹ quantum number I . The difference in mass arises because the positively charged proton interacts differently in electromagnetic interaction than the neutrally charged neutron. A few years later, in 1935, Yukawa proposed that the force of the strong interaction, the nuclear force, could be generated by the exchange of a (then hypothetical) spinless particle whose mass would have to lie between the mass of the proton and the mass of the electron. This particle was later found and is now known as the π -meson (pion). In the 1930s and 1940s, scientists developed a good understanding of the nuclear force by considering non-relativistic potential models that are attractive at long distances but repulsive at short distances, such as the Paris potential, the Bonn potential, or the shell model of the nucleus. As experiments became more extensive, it was possible to study relativistic collisions that could not be described by these non-relativistic potentials. Attempts were made between 1935 and 1965 to formulate a theory of the strong interaction based on elementary fields for baryons and mesons. However, none of these attempts proved successful. The occurring coupling constants turned out to be numerically large, indicating that ignoring higher-order contributions was not justified and perturbation theory is inapplicable. Nothing worked even a little bit.

However, it should be mentioned that great progress has been made with respect to concepts in quantum field theory, including but not limited to Lorentz invariance, crossing symmetry, causality, the CPT theorem, and renormalization. The renormalization procedure, which is necessary for obtaining physically meaningful results, had been viewed

¹Heisenberg regards the proton and neutron as two states of a particle that transform into each other under the group $SU(2)$, similar to the spin-up and spin-down states for the electron.

suspiciously by many and its validity is in question.

Gell-Mann and independently Nakano and Nishijima introduced a new quantum number to describe the so-called *strange* particles, such as the Kaon K , as additional experimental data was obtained and more particles were detected. These strange particles appear as stable particles on the time scale of the strong interaction but decay at the relatively slow time scale of the weak interaction. This new quantum number is known as the *strangeness* quantum number S . Since the number of nucleons is conserved in a nuclear reaction, the *baryon* quantum number B was additionally introduced as a bookkeeping device. This was a crucial step in organizing the numerous discovered particles, which were referred to as the particle zoo [7]. That led to the Gell-Mann-Nishijima formula (2.1) in its original form

$$Q = I_3 + \frac{1}{2}(B + S). \quad (2.1)$$

It should be noted that the electric charge Q , baryon quantum number B , and the strangeness quantum number S are conserved in all hadron reactions. However, it is worth mentioning that strangeness S is not conserved in weak interactions and the sum of $B + S$ is referred to as hypercharge Y .

During that time, the strong interaction was characterized by an energy gap in the hadron energy spectrum. The lightest state, the pion with a mass of $M_\pi \approx 135$ MeV, is much lighter than the proton which has a mass of $M_p \approx 938$ MeV. In 1960, Nambu connected that energy gap to a spontaneously broken (continuous global) symmetry². This symmetry had some generators with negative parity and is therefore referred to as *chiral symmetry*. The axial part of the symmetry is spontaneously broken, resulting in the appearance of massless particles known as Nambu-Goldstone bosons. In general, by the Goldstone Theorem³, the number of Nambu-Goldstone bosons corresponds to the number of broken generators in a spontaneously broken continuous symmetry. Therefore, the axial vector current plays an important role in determining the strength of the interaction between pions and nucleons.

If chiral symmetry were an exact symmetry, the pions as the role of the Nambu-Goldstone boson would be massless. Since they are not massless, chiral symmetry must be only an approximate symmetry.

Gell-Mann and Ne'eman independently recognized that the Gell-Mann-Nishijima formula (2.1) can be expressed as the sum of two commuting generators of the $SU(3)_f$ group. [9, 10]. These generators correspond to isospin I and hypercharge Y , and paved the way for the Eight-fold way depicted in (Fig. 2.1, Fig. 2.2).

Assuming that $SU(3)_f$ is a precise symmetry of the strong interaction while neglecting the impacts of electromagnetism and weak interactions.

In 1964, Gell-Mann and Zweig independently observed a pattern in the observed quantum numbers of mesons and baryons by considering a different representation of the (approximate) $SU(3)_f$ symmetry. This representation consists of three states and their

²In quantum field theory, the ground state (vacuum) must be invariant under the same symmetry as the underlying Lagrangian to ensure that the Lagrangian's solutions (fields) are also invariant under the symmetry. If this is not the case, we refer to it as spontaneously broken symmetry.

³The goldstone Theorem was formulated after the discovery of the Nambu-Goldstone Bosons [8].

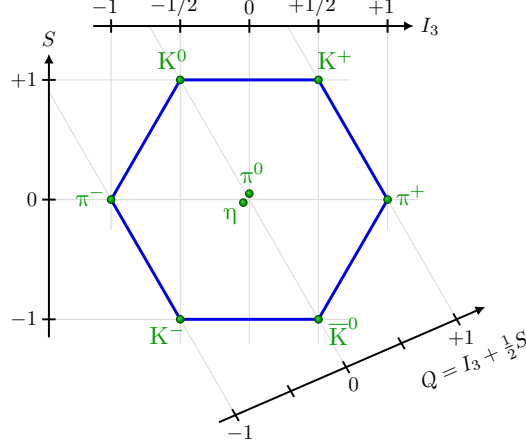


Figure 2.1: The pseudoscalar and vector mesons are organized in the Eight-fold way by the octet representation of $SU(3)$ [11]

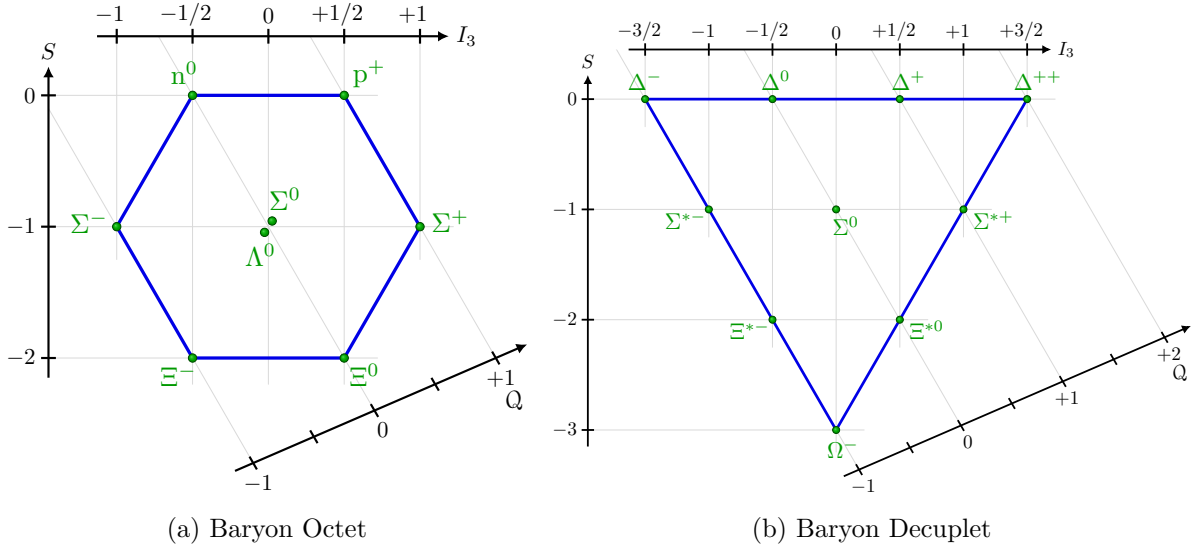


Figure 2.2: The Baryons are organized by the (a) Baryon Octet and (b) decuplet representations of $SU(3)$ [11]

conjugates, upon which every other representation can be built. These states were proposed to correspond to elementary point-like spin $1/2$ Dirac fermions, which Gell-Mann named quarks (now the standard nomenclature) and Zweig named aces. The quark model defines baryons as a bound state of three quarks (qqq) and mesons as a bound state of a quark with an antiquark ($\bar{q}q$). The model refers to the three different states as *flavors* of quarks. At that time, the known flavors of quarks were the up-quark (u), down-quark (d) and strange-quark (s) and $SU(3)_f$ isospin symmetry was thought as an exact symmetry of the strong interaction. The Eight-fold way is the generalisation of $SU(2)_f$ isospin symmetry of up-quarks (u) and down-quarks (d) to the $SU(3)_f$ isospin symmetry of up-quarks (u), down-quarks (d) and strange-quarks (s). The quark model has been highly successful. It predicted new hadronic states and explained the strengths of electromagnetic and weak interaction transitions among different hadrons. Although the original quark model was phenomenological successful, it had some controversial features and flaws:

- As baryons have a baryon quantum number of $B = 1$, each quark must have a baryon quantum number of $\frac{1}{3}$. The charges of the quarks are determined by the Gell-Mann-Nishijima formula (2.1), which states that the up-quark u has a charge of $\frac{2}{3}e^-$, while the down-quark d and strange-quark s have charges of $-\frac{1}{3}e^-$. This concept of particles carrying fractional charge in units of the electric charge was initially obscure and difficult to accept.
- The quarks were considered as mathematical auxiliary fields, because they had not been observed experimentally.
- The constituent description of the Ω_- , which is built out of 3 strange quarks (sss) appeared to contradict the Pauli-principle as 3 fermions were in the same state.
- Quarks are fermions and must obey Fermi-Dirac statistics, which means they must be anti-symmetric upon interchanging two quarks. However, the Δ^{++} particle is composed of three up-quarks (uuu) and has a spin of $s_z = 3/2$, making it symmetric in flavor and spin. Therefore, the spatial wave function must be antisymmetric. However, the spatial wave functions ground state is symmetric for every reasonable potential, which leads to a contradiction.

Bogolyubov, Struminsky and Tavkhelidze [12], Han and Nambu [13] and Miyamoto [14] independently discovered that quarks must exist in three different states to overcome the challenges of the quark model. Murray Gell-Mann introduced the term *color* as an additional quantum number. It transforms under the group $SU(3)_c$. The three color state of the quarks are commonly called *red*, *green* and *blue* state. Nambu proposed that the forces between colored quarks are mediated by the $SU(3)_c$ octet, which consists of eight *gluons*. This concept is similar to the role of the photon in mediating the forces between charged particles in quantum electrodynamics (QED) [15]. With the introduction of color, charged quarks can occupy the same energy state while being in different color states, thus satisfying the Pauli principle. To ensure compatibility with Fermi-Dirac statistics, the quark wavefunction must be completely anti-symmetric in color quantum number. Hence, quarks carry two indices: flavor and color. The MIT-SLAC experiment confirmed the presence of point-like structures inside protons, supporting the underlying theory. Feynman referred to these point-like structures as *partons* to leave it open whether they are the emphasized quarks or something else. The primary objective at this stage was to identify the appropriate theoretical framework that satisfies all the collected information. In the 1970s, physicists developed a non-Abelian gauge theory to describe the interactions between quarks and gluons. David J. Gross, Frank Wilczek, and David Politzer were awarded the Nobel Prize for their demonstration that these non-Abelian gauge theories are asymptotically free, meaning that the interaction between quarks and gluons weakens at high energies (small distances) and perturbation theory is justified. Another crucial aspect to consider in the theory of strong interaction is *confinement*. This refers to the fact that quarks and gluons cannot exist as free particles, but only as color-neutral bound states known as hadrons. It is noteworthy that Gerard 't Hooft had previously reached a similar conclusion about the asymptotically free nature of non-Abelian gauge theories, but chose not to publish his findings until progress had been made on the quark confinement problem, as documented in [16]. The energy gap in the hadron spectrum can now be attributed to the breaking of the approximate $SU(3)_f$ isospin symmetry, which is caused by the strange quark being more massive than the up-quark (u) and down-quark (d). Through the global and local gauge invariance of the exact $SU(3)_c$ symmetry

in a non-Abelian gauge theory regime, the theory of the strong interaction, known as *Quantum Chromodynamics* (QCD), was developed by H. Fritzsch, M. Gell-Mann and H. Leutwyler [17]. The journey from the quark model to asymptotic freedom and quark confinement leading to QCD, is a remarkable story of scientific discovery. For a review see [18–20]

In summary, the quark theory proposed by Gell-Mann and Zweig has been confirmed as an accurate description of the strong interaction. The theory involves quarks with fractional electric charges that interact via an octet of gauge fields known as gluons in the $SU(3)_c$ color group. Within this framework, partons are identified as quarks that always remain confined in hadrons. Gell-Mann named this renormalizable quantum field theory QCD. Over time, experimental discoveries have led to the identification of heavier quarks, namely charmed (c), top (t), and bottom (b). Today’s standard model is based on three quark doublets or generations: (u, d) , (c, s) , and (t, b) , each associated with increasing mass. This development has solidified QCD as a fundamental component of our understanding of the strong force and the intricate dynamics of subatomic particles [9].

2.2 QCD Lagrangian

So far, we have acquired an asymptotically free and non-Abelian gauge theory built on the structure group $SU(3)_c$ of quark and gluon fields. The key feature that sets gluons apart from photons, acting as gauge bosons, is their possession of color charge, enabling them to self-interact. This attribute gives rise to a complex theory with numerous non-perturbative phenomena and therefore non-perturbative methods are essential to explore these phenomena. The article utilizes an approach that employs functional methods, as presented in [21–25]. The article uses correlation functions linked to generating functionals as its fundamental building blocks.

First, we want to introduce explicitly the Lagrangian density of QCD in the Euclidean convention⁴, as presented in [26].

$$\mathcal{L}_{QCD} = \frac{1}{2} \text{tr}_c [F_{\mu\nu} F_{\mu\nu}] + \sum_f \bar{q}^{(f)} (\not{D} + m^{(f)}) q^{(f)}. \quad (2.2)$$

In this expression the *covariant derivative* D_μ in $\not{D} = \gamma_\mu D_\mu$ is defined as

$$D_\mu = \partial_\mu + ig A_\mu, \quad (2.3)$$

where A_μ represents the gluon fields and g is the strong coupling constant. The gluon fields A_μ follow the $\mathfrak{su}(3)$ Lie algebra in the adjoint representation, which satisfies the commutation relation

$$[t^a, t^b] = if^{abc} t^c. \quad (2.4)$$

Here, f^{abc} represents the totally antisymmetric structure constants of the group $SU(3)$, similar to the Levi Civita tensor ε_{abc} for the group $SU(2)$. The generators fulfill the standard normalization

⁴For more information see App. A.1

$$\text{tr}_c [t^a t^b] = \frac{\delta^{ab}}{2}. \quad (2.5)$$

t^a represents the eight generators of the group. These generators are connected to the Gell-Mann matrices λ^a by $t^a = \lambda^a/2$. This means that the gluon field A_μ can be decomposed as $A_\mu = \sum_{a=1}^8 A_\mu^a t^a$.

The color trace explicitly reads $\frac{1}{2} \text{tr}_c [F_{\mu\nu} F_{\mu\nu}] = \frac{1}{4} F_{\mu\nu}^a F_{\mu\nu}^a$, where $F_{\mu\nu}$ is the gluon field strength tensor defined as

$$F_{\mu\nu} := -\frac{i}{g} [D_\mu, D_\nu] = \partial_\mu A_\nu - \partial_\nu A_\mu + ig[A_\mu, A_\nu] \quad (2.6)$$

Therefore, the gluon field strength tensor $F_{\mu\nu}$ inherits the same decomposition in the $\text{su}(3)$ Lie algebra, meaning that $F_{\mu\nu} = \sum_a F_{\mu\nu}^a t^a$ and $F_{\mu\nu}^a$ can be written as

$$F_{\mu\nu}^a = \partial_\mu A_\nu^a - \partial_\nu A_\mu^a - gf^{abc} A_\mu^b A_\nu^c. \quad (2.7)$$

The fields \bar{q} and q represent the Dirac antiquark and quark fields for each quark flavor f , where $f \in \{u, d, s, c, b\}$. The mass term $m^{(f)}$ in the Lagrangian (2.2) is matrix-valued and should be read as $m^{(f)} \mathbb{1}_c$. These are the *current-quark masses*⁵ and are input parameters of our theory. As this thesis focuses on the pion, only the u and d quarks are considered. The mass difference between the u and d quarks is only a few MeV, hence we work in the isospin limit where $m^{(u)} = m^{(d)} = m$ holds.

2.3 Gauge fixing

The Lagrangian in (2.2) is constructed to be locally and globally invariant with respect to $\text{SU}(3)_c$ gauge transformations, but it has a major issue. If non-perturbative methods are used, e.g. functional methods such as the Dyson-Schwinger equations, it is observed that the gluon propagator does not exist, because it is proportional to a transverse projector, which is not invertible (having vanishing eigenvalues). The issue of gauge invariance also arises in QED with the photon propagator. To address this, the Gupta-Bleuler procedure is used in QED to cure this problem. In QCD, the most common method is the Faddeev-Popov procedure, which involves breaking gauge invariance in the Lagrangian⁶ by fixing a gauge using a gauge condition. The gauge typically used and will be used here is the *linear covariant gauge* with the gauge condition $\partial_\mu A_\mu^a = 0$. In the most common manner the Lagrangian \mathcal{L}_{QCD} is replaced by

$$\mathcal{L}_{QCD} \rightarrow \mathcal{L}_{QCD} + \mathcal{L}_{GF} = \mathcal{L}_{QCD} + \frac{1}{2\xi} (\partial_\mu A_\mu^a(x))^2 + \bar{c}^a(x) (\partial_\mu D_\mu^{ab}) c^b(y). \quad (2.8)$$

The first term of the additional Lagrangian \mathcal{L}_{GF} employs our gauge condition with a real Lagrange multiplier $\lambda := \frac{1}{\xi}$, where ξ is used as the gauge parameter. The second term of

⁵The current-quark mass, also known as the bare quark mass, refers to the mass of a quark that arises due to its Yukawa interaction with the Higgs field. In contrast, when a quark is bound, it continuously exchanges gluons with its counterparts in the bound state. This process increases the total energy of the hadron, resulting in a larger mass. This is known as the constituent quark mass [27].

⁶Fixing the gauge in the Lagrangian is necessary, when employing methods such as Dyson-Schwinger equations, since they rely on unobservable propagators like the quark or gluon propagator

\mathcal{L}_{GF} introduces an auxiliary field called ghost field c to handle the non-trivial determinant that occurs in the Fadeev-Popov procedure. The ghost field is negative-definite and therefore unphysical. Using the Ward-Takahashi identity, it has been proved that the experimentally measurable S-matrix is independent of ξ . Therefore, observables such as masses and decay widths are gauge-independent (independent of ξ), even though the Green's functions are now gauge-dependent. For simplicity, we work in the Landau gauge, where $\xi = 0$. This has the advantage that the longitudinal part of the gluon propagator vanishes. This paragraph gives a brief summary of the necessity and implications of the Fadeev-Popov procedure. For a detailed review containing in-depth calculations, see [28].

2.4 Generating DSE for 1PI correlation functions

This section provides a brief introduction to the basic objects used in quantum field theory when applying the scheme of the path integral quantization in the Euclidean convention as described in App. A.1.

Similar to statistical physics, the physical content of a quantum field theory is derived from its partition function Z . The partition function $Z[0]$ is defined as

$$Z[0] = \int \mathcal{D}\varphi e^{-S[\varphi]} = \lim_{n \rightarrow \infty} \int d\varphi(x_1) \dots d\varphi(x_n) e^{-S[\varphi]}, \quad S[\phi] = \int d^4x \mathcal{L}[\phi], \quad (2.9)$$

and will be the starting point. Herein, $S[\varphi]$ is the classical action. The integral measure in (2.9) can be understood as the integration over all possible field configurations $\varphi(x)$ at each spacetime coordinate x_i . Each field configuration is weighted with $e^{-S[\varphi]}$ as a probability measure. The partition function is therefore the implementation of the quantum corrections necessary for the classical path⁷.

By analogy with classical physics, where the object of interest is the trajectory, the objects of interest in quantum field theory are the *correlation functions* or *Green's functions*. The Green's functions are given by the (vacuum) expectation values of the time-ordered fields.

$$G^{(n)}(x_1, \dots, x_n) = \langle 0 | T \varphi(x_1) \dots \varphi(x_n) | 0 \rangle = \frac{1}{Z[0]} \int \mathcal{D}\varphi \varphi(x_1) \dots \varphi(x_n) e^{-S[\varphi]}. \quad (2.10)$$

The expectation value in this context refers to the field φ that originates at point x_1 and propagates to points x_2 , x_3 , and so on, until reaching x_n . It is crucial to differentiate between the φ inside the expectation value, which acts as field operators on the vacuum $|0\rangle$, and the φ inside the path integral, which are functions.

The Green's functions can be also generated by the partition function $Z[J]$ by a mathematical trick. Here we add an external source term $S_s[J] = \int d^4x \varphi(x) J(x)$ to the classical action in the path integral

$$Z[J] = \int \mathcal{D}\varphi e^{-S[\varphi] + S_s[J]}, \quad S_s[J] = \int d^4x \varphi(x) J(x). \quad (2.11)$$

Then we differentiate the Functional $Z[J]$ with respect to the source $J(x_1)$ to obtain

$$\frac{\delta Z[J]}{\delta J(x_1)} = \int \mathcal{D}\varphi \varphi(x_1) e^{-S[\varphi] + S_s[J]}. \quad (2.12)$$

⁷The classical path is defined by the Euler-Lagrange equation originating from $\frac{\delta S[\varphi]}{\delta \varphi} = 0$.

After differentiation, we set the source $J \rightarrow 0$:

$$\left. \frac{\delta Z[J]}{\delta J(x_1)} \right|_{J=0} = \int \mathcal{D}\varphi \varphi(x_1) e^{-S[\varphi]} = Z[0] \langle 0 | T \varphi(x_1) | 0 \rangle := Z[J] G_J^{(1)}(x_1) \Big|_{J=0}. \quad (2.13)$$

This procedure pathed a way to obtain the full one-point Green's function from the generating functional $Z[J]$. Generalizing these procedure by combining (2.10) and (2.13), we obtain for the n -point Green's function

$$G^{(n)}(x_1, \dots, x_n) = \frac{1}{Z[J]} \frac{\delta}{\delta J(x_1)} \cdots \frac{\delta}{\delta J(x_n)} Z[J] \Big|_{J=0}. \quad (2.14)$$

The objects that enter the S-matrix are the *connected* Green's functions $G_{\text{conn}}^{(n)}$ and therefore of great theoretical interest. They can be obtained by taking functional derivatives of the generating functional for connected Green's function $W[J] = \ln Z[J]$. They read explicitly as

$$G_{\text{conn}}^{(n)}(x_1, \dots, x_n) = \frac{\delta}{\delta J(x_1)} \cdots \frac{\delta}{\delta J(x_n)} W[J] \Big|_{J=0}. \quad (2.15)$$

In this expression, we made the implicit assumption that $Z[0] = 1$ and is therefore properly normalized. An explicit calculation of the connected two-point Green function

$$\begin{aligned} G_{\text{conn}}^{(2)}(x_1, x_2) &= \frac{\delta}{\delta J(x_1)} \frac{\delta}{\delta J(x_2)} W[J] \Big|_{J=0} \\ &= \frac{\delta}{\delta J(x_1)} \frac{\delta}{\delta J(x_2)} \ln Z[J] \Big|_{J=0} \\ &= \frac{\delta}{\delta J(x_1)} \left(\frac{1}{Z[J]} \int \mathcal{D}\varphi \varphi(x_2) e^{-S[\varphi] + \int d^4x \varphi(x) J(x)} \right) \Big|_{J=0} \\ &= \frac{1}{Z[J]} \frac{\delta^2 Z[J]}{\delta J(x_2) \delta J(x_1)} \Big|_{J=0} - \frac{1}{Z^2[J]} \frac{\delta Z[J]}{\delta J(x_1)} \frac{\delta Z[J]}{\delta J(x_2)} \Big|_{J=0} \\ &= \frac{\delta^2 Z[J]}{\delta J(x_1) \delta J(x_2)} \Big|_{J=0} - \frac{\delta Z[J]}{\delta J(x_1)} \frac{\delta Z[J]}{\delta J(x_2)} \Big|_{J=0}, \end{aligned} \quad (2.16)$$

shows that the general structure of the connected Green's function plays a role analogous to the cumulants or moments of a probability distribution. In this example, it becomes apparent why the nomenclature is chosen as the connected Green's function. Schematically the structure of $G_{\text{conn}}^{(n)}(x_1, \dots, x_n)$ is 'all connected diagrams - all disconnect diagrams'.

Next, we introduce the *one-particle-irreducible* (1PI) Green's functions. The generating functional for the 1PI Green's functions $\Gamma[\Phi]$ is defined by the Legendre transform of $W[J]$ denoted as

$$\Gamma[\Phi] = -W[J] + \int d^4x \Phi(x) J(x). \quad (2.17)$$

Furthermore, we can link all three generating functionals via

$$Z[J] = \int \mathcal{D}\varphi e^{-S[\varphi] + \int d^4x \varphi(x)J(x)} = e^{W[J]} = e^{-\Gamma[\Phi] + \int d^4x \Phi(x)J(x)}. \quad (2.18)$$

Furthermore the fields φ and Φ can be put into relation by considering

$$\langle \varphi(x) \rangle_J = \frac{1}{Z[J]} \frac{\delta}{\delta J(x)} Z[J] = \frac{\delta}{\delta J(x)} \ln Z[J] = \frac{\delta}{\delta J(x)} W[J] = \Phi(x). \quad (2.19)$$

Therefore the field Φ is the expectation value of the field φ in the presence of the source J . Note that for $\Gamma[\Phi]$, also called the *quantum effective action* in (2.17), the source is the averaged field $\langle \varphi(x) \rangle_J$. The 1PI Green's functions are therefore

$$G_{\text{1PI}}^{(n)}(x_1, \dots, x_n) := \Gamma^{(n)}(x_1, \dots, x_n) = \frac{\delta}{\delta \Phi(x_1)} \dots \frac{\delta}{\delta \Phi(x_n)} \Gamma[\Phi] \Big|_{\Phi=0} \quad (2.20)$$

The *propagator* is defined as $(\Gamma^{(2)}(x_1, x_2))^{-1} = G_{\text{conn}}^{(2)}(x_1, x_2) := D(x_1, x_2)$, where the relation in the first equality can be shown by

$$\begin{aligned} G_{\text{conn}}^{(2)}(x_1, x_2) \Gamma^{(2)}(x_1, x_2) &= \frac{\delta^2 W[J]}{\delta J(x_1) \delta J(x_2)} \frac{\delta^2 \Gamma[\Phi]}{\delta \Phi(x_1) \delta \Phi(x_2)} \\ &= \frac{\delta^2 W[J]}{\delta J(x_1) \delta J(x_2)} \frac{\delta J(x_2)}{\delta \Phi(x_1)} \\ &= \frac{\delta^2 W[J]}{\delta J(x_1) \delta \Phi(x_1)} \\ &= \frac{\delta \Phi(x_1)}{\delta \Phi(x_1)} \\ &= 1. \end{aligned} \quad (2.21)$$

The 1PI Green's function has a diagrammatical meaning that ensures the remaining diagram to not become disconnected upon cutting a single line, assuming that external lines are amputated. This allows for the expansion of any full correlation function in terms of 1PI correlation functions, preventing overcounting of diagrams.

We can generalize (2.14) for any polynomial expectation value of the field φ by defining $P[\varphi]$ as the polynomial functional. The Green's function can therefore be written as

$$\begin{aligned} \langle P[\varphi] \rangle_J &= Z^{-1}[J] P \left[\frac{\delta}{\delta J} \right] Z[J] \\ &= e^{-\ln Z[J]} P \left[\frac{\delta}{\delta J} \right] e^{\ln Z[J]} \\ &= e^{-W[J]} P \left[\frac{\delta}{\delta J} \right] e^{W[J]} \\ &= P \left[\frac{\delta}{\delta J} + \frac{\delta W[J]}{\delta J} \right] \end{aligned} \quad (2.22)$$

In this notation, for example, the expression $P \left[\frac{\delta}{\delta J} \right]$ is understood to represent the replacement of all fields φ with the expression in the bracket. We can further express the

functional derivative of the source J in terms of the propagator D as

$$\begin{aligned}\frac{\delta}{\delta J(x)} &= \int d^4z \frac{\delta \Phi(z)}{\delta J(x)} \frac{\delta}{\delta \Phi(z)} \\ &= \int d^4z \frac{\delta}{\delta J(x)} \frac{\delta W[J]}{\delta J(z)} \frac{\delta}{\delta \Phi(z)} \\ &= \int d^4z D(x, z)_J \frac{\delta}{\delta \Phi(z)},\end{aligned}\tag{2.23}$$

where $D(x, z)_J$ indicates that the propagator is still source dependent. Plugging (2.23) into (2.22) using that $\frac{\delta W[J]}{\delta J(x)} = \Phi(x)$, yields

$$\langle P[\varphi] \rangle_J = P \left[\Phi(x) + \int d^4z D(x, z)_J \frac{\delta}{\delta \Phi(z)} \right]. \tag{2.24}$$

We are only one step away from the Dyson-Schwinger equation for 1PI correlation functions. The missing link is the fact that the total derivative of $Z[J]$ vanishes

$$0 = \int \mathcal{D}\varphi \frac{\delta}{\delta \varphi(x)} e^{-S[\varphi] + \int d^4y \varphi(y) J(y)} = \int \mathcal{D}\varphi \left(-\frac{\delta S[\varphi]}{\delta \varphi(x)} + J(x) \right) e^{-S[\varphi] + \int d^4y \varphi(y) J(y)},$$

reordering the terms gives

$$\left\langle \frac{\delta S[\varphi]}{\delta \varphi(x)} \right\rangle_J = \langle J(x) \rangle_J = J(x) = \frac{\delta \Gamma[\varphi]}{\delta \Phi(x)} \tag{2.25}$$

using (2.24) in (2.25) we obtain the generating Dyson-Schwinger equation in terms of the 1PI correlation functions

$$\frac{\delta \Gamma[\varphi]}{\delta \Phi(x)} = \frac{\delta}{\delta \varphi(x)} S \left[\Phi(x) + \int d^4z D(x, z)_J \frac{\delta}{\delta \Phi(z)} \right] \tag{2.26}$$

By further differentiation of (2.26) we get the propagator or vertices of various quantities.

The Feynman rules for W are identical to those for Z , with the exception that only connected diagrams are summed. This is because all contributions from corrections to the denominator $Z[0]$ are disconnected, and therefore do not need to be considered. Those familiar with statistical mechanics will recognize the relationship between Z and W to be analogous to that between the partition function and the Helmholtz free energy, particularly in Euclidean QFT, as demonstrated here this analogy is exact. Upon returning to Minkowski space, a factor of i and -1 will be encountered in this analogy.

Vertex functions, which are defined by functional derivatives of 1PI Green functions, have been also referred to as proper correlation functions and one-particle-irreducible correlation functions. Diagrammatically, 1PI correlation functions are constructed as the sum of all diagrams that cannot be cut into disconnected parts by cutting a single propagator line. At the tree level, these simply represent the vertices constructed from the classical action. This is the reason why it is also called the quantum effective action. The exact momentum-space two-point function⁸, $(\Gamma^{(2)}(p))^{-1}$, has a pole at the mass of any stable particle that can be created from the vacuum by the quantum field. This generalizes and motivates the usage of the 1PI expansion of n -point connected Green functions.

⁸Note that after setting $J = 0$ the two-point function is translation invariant and its Fourier transformation into momentum space depends only on one variable

Chapter 3

Quark DSE

In the last section, the generating Dyson-Schwinger equation (or master equation) for the 1PI Green's functions was derived. With the master equation at hand, we will consider the quantity

$$\left(\frac{\delta^2 \Gamma}{\delta \bar{q}^i(x) \delta q^j(y)} \right)^{-1} \Big|_{q=0} := S^{ij}(x, y), \quad (3.1)$$

which defines the DSE for the Quark Propagator.

Upon performing the calculation and Fourier transforming into momentum space we can read off the DSE for the quark propagator $S(p)$ in its diagrammatic form as shown in Fig. 3.1.

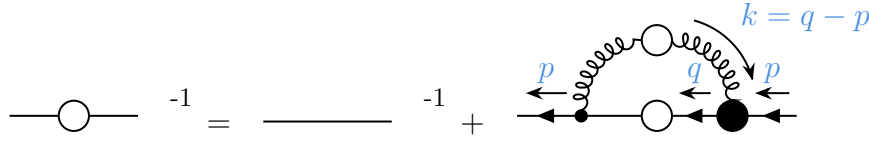


Figure 3.1: Diagrammatic Quark Propagator DSE

Quantities with an empty blob denote dressed quantities such as the dressed quark propagator and the dressed gluon propagator. The thin blob denotes a bare quark-gluon vertex, while the thick blob denotes a dressed quark-gluon vertex. The DSE for the Quark propagator can therefore be expressed as follows:

$$S^{-1}(p) = S_0^{-1}(p) + \Sigma(p). \quad (3.2)$$

Here, $S_0(p)$ represents the tree-level quark propagator, while $\Sigma(p)$ is referred to as the self energy, accounting for quantum loop corrections. For the sake of simplicity, we shall reconstruct the explicit form of the full quark propagator $S^{-1}(p)$, by employing the renormalized Euclidean Feynman rules for QCD, which are stated in App. B.1. We shall then apply these rules to the diagrammatic quark propagator DSE in Fig. 3.1. This procedure yields the result

$$S^{-1}(p) = Z_2(i\not{p} + m_0) - \frac{4g^2}{3} Z_{1f} \int \frac{d^4 q}{(2\pi)^4} i\gamma^\mu S(q) D^{\mu\nu}(k) \Gamma^\nu(l, k), \quad (3.3)$$

where the prefactor $\frac{4}{3}$ originates from the color trace of the self energy term, which is explicitly calculated in App. D.1. Note that the full quark-gluon vertex $\Gamma^\mu(l, k)$ depends on the gluon momentum $k = q - p$ and the relative gluon momentum $l = \frac{p+q}{2}$.

However, the quark propagator $S(p)^{-1}$ can also be expanded into a tensorial basis consisting of $\{\mathbb{1}, \not{p}\}$. Given that the bare quark propagator $S_0^{-1}(p)$ is already expressed in terms of the tensorial basis mentioned, it follows that the self-energy $\Sigma(p)$ must also be expanded into the same basis. This results in the following equations:

$$S^{-1}(p) = A(p^2) (i\not{p} + M(p^2)), \quad \Sigma(p) = \Sigma_A(p^2) i\not{p} + \Sigma_M(p^2). \quad (3.4)$$

This leads to the coupled integral equations for the dressing functions $A(p^2)$ and $M(p^2)$:

$$\begin{aligned} A(p^2) &= Z_2 + \Sigma_A(p^2), \\ A(p^2)M(p^2) &= Z_2 m_0 + \Sigma_M(p^2). \end{aligned} \quad (3.5)$$

The self-energy dressing functions $\Sigma_A(p^2)$ and $\Sigma_M(p^2)$ can be obtained by taking Dirac traces

$$\begin{aligned} \Sigma_M(p^2) &= \frac{1}{4} \text{Tr} [\Sigma(p)], \\ \Sigma_A(p^2) &= \frac{1}{4p^2} \text{Tr} [-i\not{p} \Sigma(p)]. \end{aligned} \quad (3.6)$$

Before proceeding, we introduce a truncation scheme to overcome the intricacies of the full quark-gluon vertex, $\Gamma^\nu(l, k)$. One popular choice is the so-called *rainbow-ladder truncation* (RL truncation), which will be employed here and which can be found in the App. C.1 for further information.

Upon implementing the RL truncation we arrive at

$$\Sigma(p) = \frac{4g^2}{3} Z_{1f} \int \frac{d^4 q}{(2\pi)^4} \frac{Z(k^2)}{k^2} f(k^2) T_k^{\mu\nu} \gamma^\mu S(q) \gamma^\nu, \quad (3.7)$$

for the self energy. Furthermore, we employ an effective interaction $\alpha(k^2)$ using the Maris-Tandy model [29], with more information in App. C.2,

$$\alpha(k^2) = \frac{g^2}{4\pi} \frac{Z_{1f}}{Z_2^2} Z(k^2) f(k^2) = \pi \eta^7 \left(\frac{k^2}{\Lambda^2} \right)^2 e^{-\eta \frac{k^2}{\Lambda^2}} + \alpha_{UV}. \quad (3.8)$$

In this thesis the ultraviolet term α_{UV} is neglected. The first term provides a description of the infrared region and is responsible for the dynamical generation of a quark mass. This term is relatively insensitive to variations in the value of η between 1.6 and 2. The value of $\eta = 1.8$ was chosen arbitrarily. With this simplification, we can easily take the Dirac traces in (3.6). Since the self-energy integrals are logarithmically UV-divergent, a renormalization must be employed. This is achieved by demanding

$$\begin{aligned} A(\mu^2) &\stackrel{!}{=} 1 \iff Z_2 = 1 - \Sigma_A(\mu^2), \\ M(\mu^2) &\stackrel{!}{=} m \iff m_0 = \frac{m - \Sigma_M(\mu^2)}{1 - \Sigma_A(\mu^2)}, \end{aligned} \quad (3.9)$$

where μ^2 is the arbitrary renormalization point.

The final form of the quark DSE is then given by

$$\begin{aligned} A(p^2) &= 1 + \Sigma_A(p^2) - \Sigma_A(\mu^2), \\ M(p^2)A(p^2) &= m + \Sigma_M(p^2) - \Sigma_M(\mu^2). \end{aligned} \quad (3.10)$$

Since the ultraviolet correction term α_{UV} has been omitted from the effective interaction $\alpha(k^2)$, it is now possible to calculate the integration over z analytically. This reduces the numerical effort to a single momentum integration over q^2 . The explicit expressions for the self energy dressing functions after analytically integrating over z is found in App. D.4. The momentum integration was performed numerically using a Gauss-Legendre procedure with 300 grid points. The integration cutoff was set to be

$$\int_0^\infty dq^2 \rightarrow \int_0^{L^2=10^6 \text{ GeV}^2} dq^2 \quad (3.11)$$

It is understood that this is an iterative procedure, where the updated values of $A(p^2)$, $M(p^2)$ and Z_2 are calculated after each iteration. The renormalized current-quark mass m , is an input parameter. Since we are working in the isospin limit, both up and down quarks have the same mass. A characteristic value is $m = 4 \text{ MeV}$.

The renormalization constant $Z_2(\mu^2)$ is used to relate the bare dressing function $A_{bare}(p^2)$ to the renormalized one by the equation $A_{bare}(p^2) = \frac{1}{Z_2(\mu^2)} A(p^2, \mu^2)$. Consequently, the dressing function $\frac{1}{A(p^2)}$ is also referred to as the quark wave function renormalization. Due to the absence of a renormalization constant relating the bare mass function M_{bare} to the renormalized one M , the mass function remains independent of the renormalization point $M_{bare}(p^2) = M(p^2)$. This implies that the interpretation of $M(p^2)$ as a running quark mass is acceptable. A value of $\mu^2 = 19 \text{ GeV}^2$ was chosen as it is a frequently employed choice in the literature, e.g. [30].

It can be demonstrated that once the equations have been iterated until convergence, the inputs from the complex plane can be used for the Euclidean momenta, as previously demonstrated in the literature [31]. This is due to the fact that there are no poles in the region of interest for our study of Bethe-Salpeter equations, which is discussed in [32]. This is of great importance since the quark propagator in the complex plane is needed for the study of the Bethe-Salpeter equations. The absence of poles in our region of interest can be related to the choice of the prefactor k^4 in the effective interaction in (C.2). The quark dressing functions are therefore calculated at the exact input, eliminating the necessity for any fitting or interpolation.

Chapter 4

Pion BSE

In order to extract properties from the pion as a quark-antiquark bound state, we will first introduce the four-point Green's function $G^{(4)}$ of two quarks and two antiquarks. This is defined as $G^{(4)} = \langle 0 | q_1 q_2 \bar{q}_3 \bar{q}_4 | 0 \rangle$. Poles in the Green function correspond to bound states, in this case, a meson. In principle this also includes resonances. When the total four-momentum of the meson P goes on shell $P^2 = -M^2$ the Green's function behaves like

$$G^{(4)} \sim \frac{\Psi \bar{\Psi}}{P^2 + M^2}, \quad (4.1)$$

where Ψ is called the Bethe-Salpeter wave functions. Alternatively, it can be formulated with the *scattering matrix* $T^{(4)}$, which accounts for all possible two-on-two quark-antiquark scattering processes:

$$T^{(4)} \sim \frac{\Gamma \bar{\Gamma}}{P^2 + M^2}. \quad (4.2)$$

Here, Γ is called the *Bethe-Salpeter amplitude* (BSA). Inserting this into the respective Dyson equations

$$G^{(4)} = G_0^{(4)} + G_0^{(4)} K^{(4)} G^{(4)} \iff T^{(4)} = K^{(4)} + K^{(4)} G_0^{(4)} T^{(4)}, \quad (4.3)$$

yields the homogeneous Bethe-Salpeter equation, which only holds at the discrete pole location $P^2 = -M^2$:

$$\Psi = G_0^{(4)} K^{(4)} \Psi \iff \Gamma = K^{(4)} G_0^{(4)} \Gamma. \quad (4.4)$$

The *four-quark scattering kernel* $K^{(4)}$ represents here the two-particle irreducible kernel with respect to the quark propagators. It should be noted that the quantities retain their full Dirac and color structure in this simplified notation, and a four-dimensional integration must be performed. For a detailed derivation, please refer to [22]. The explicit homogeneous Bethe-Salpeter equation for the pion's BSA is given by the following equation:

$$[\Gamma(P; p)]_{\alpha\beta} = \int \frac{d^4 q}{(2\pi)^4} [K^{(4)}(P; p, q)]_{\alpha\gamma, \delta\beta} [S(q_+) \Gamma(P; q) S(q_-)]_{\gamma\delta}. \quad (4.5)$$

In order to arrive at this equation, it is necessary to first define the tree-level four-point function $G_0^{(4)}$. This is demonstrated to be a disconnected product of a dressed quark and a dressed antiquark propagator, given by $G_0^{(4)} = S(q_+) \otimes S(q_-)$, where the tensor product

is taken with respect to the color, flavor and Dirac structure. A graphical depiction of the pion BSE with its momentum routing is shown in Fig. 4.1.

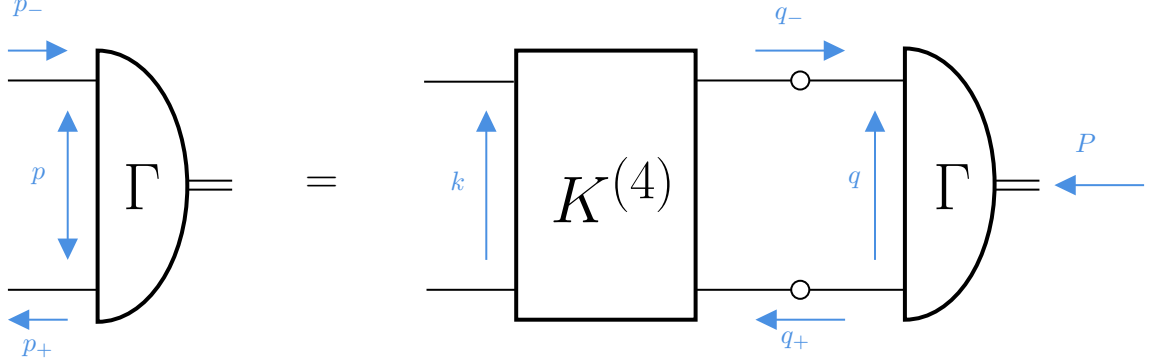


Figure 4.1: The Pion BSE with its explicit momentum routing

The momenta of the quark $q_- = q - \eta P$ and anti-quark $q_+ = q + (\eta - 1)P$ are partitioned by the parameter $\eta \in [0, 1]$, where $\eta = \frac{1}{2}$ is chosen and is said to be an optimal choice in terms of numerics. This property of the internal loop momenta demonstrates the fully Lorentz-invariant nature of the pion BSE, indicating that no specific frame is required for analysis. Nevertheless, we adopt the parametrization of the momenta as in the quark DSE using hyperspherical coordinates, with the specification that we work in the rest frame of the pion, see App. E.1.

It is at this point unclear whether the description in question refers to a pion, a ρ -meson, a scalar diquark, or any other meson. Different types of mesons are distinguished by their Dirac structure. So our task is to construct the tensorial structure of $\Gamma(P; p)$ such that it matches the property of the pion. The pseudoscalar pion carries quantum numbers $J^{PC} = 0^{-+}$. This means that we need a tensorial basis for spin $J = 0$ with negative parity and which is even under charge-conjugation $\bar{\Gamma}(P; p) = C \Gamma(-P; -p)^T C^T \stackrel{!}{=} \Gamma(-P; p)$. Here, $C = \gamma^4 \gamma^2$ is the charge-conjugation matrix. For a particle with spin $J = 0$, the set of all anti-symmetric tensors

$$\mathbb{1}, \quad \gamma^\mu, \quad [\gamma^\mu, \gamma^\nu], \dots \quad (4.6)$$

contracted with the independent momenta p for the relative quark momentum and P for the total pion momentum constitutes in principle a complete tensor basis for the particle. Consequently, the tensorial basis decomposition of the pion's Dirac structure becomes

$$\Gamma(P; p) \gamma_5 := \mathbf{\Gamma}(P; p) = (f_1 \mathbb{1} + i f_2 \not{P} + i f_3 (p \cdot P) \not{p} + f_4 [\not{p}, \not{P}]) \gamma_5. \quad (4.7)$$

The factor of γ_5 represents the practical implementation of negative parity and the factor of $(p \cdot P)$ in the third term ensures the correct behavior under charge conjugation. By convention, an extra i has been factored out in the second and third term, such that the dressing functions¹ f_i , $i = 1, \dots, 4$ become real-valued.

In order to perform a practical calculation, it is necessary to have a model for the two-particle irreducible four-quark scattering kernel $K^{(4)}$. This is because the object is too

¹In the literature the dressing functions have different nomenclature. These are as follows: $f_1 \iff E$, $f_2 \iff F$, $f_3 \iff G$, $f_4 \iff H$.

complicated to handle and no closed expression exists. However, there is a catch in that the truncation scheme cannot be arbitrary. It is constrained by the axial-vector Ward-Takahashi identity (AVWTI) [33]

$$\{\gamma^5 \Sigma(-p_-) + \Sigma(p_+) \gamma^5\}_{\alpha\beta} = - \int K_{\alpha\gamma, \delta\beta}^{(4)}(P; p, q) \{\gamma^5 S(-q_-) + S(q_+) \gamma^5\}_{\gamma\delta}. \quad (4.8)$$

This equation relates the quark self-energy to $K^{(4)}$. Only a kernel that preserves the AVWTI ensures the correct behavior in the chiral limit² of the pion, which is the Goldstone boson of QCD related to the dynamical breaking of chiral symmetry. The simplest truncation scheme fulfilling that identity is the RL truncation as described in C.1. Accordingly, the full kernel is approximated by a gluon exchange between the quark and anti-quark. This is represented by

$$K_{\alpha\gamma, \delta\beta}^{(4)}(P; p, q) = 4\pi Z_2^2 \frac{\alpha(k^2)}{k^2} (t_a)_{ij} (t_a)_{kl} (i\gamma^\mu)_{\alpha\gamma} T_k^{\mu\nu} (i\gamma^\nu)_{\delta\beta}. \quad (4.9)$$

In this equation, $T_k^{\mu\nu}$ is the transversal projector as defined in B.1 and $k = p - q$ is the momentum transferred over the gluon. The RL truncated kernel is depicted in Fig. 4.2.

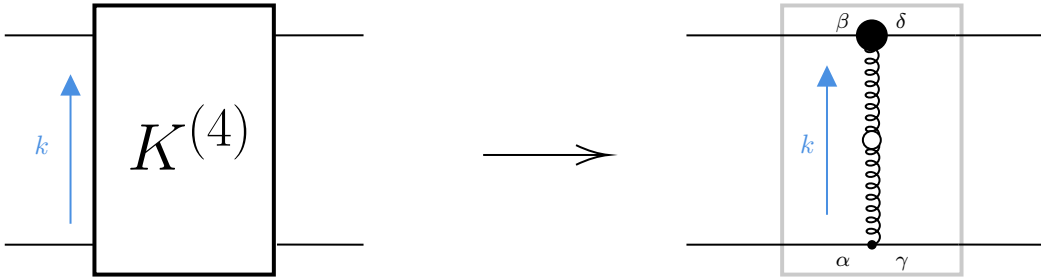


Figure 4.2: The RL truncated four-quark scattering kernel $K^{(4)}$

Upon inserting the result of equation (4.9) into equation (4.5) and multiplying with γ_5 from the right, one obtains the following result for the pion BSA

$$\Gamma(P; p) = \frac{16\pi}{3} Z_2^2 \int \frac{d^4 q}{(2\pi)^4} \frac{\alpha(k^2)}{k^2} T_k^{\mu\nu} \gamma^\mu S(q_+) \Gamma(P; q) S(-q_-) \gamma^\nu, \quad (4.10)$$

where the anticommutation relation $\{\gamma^5, \gamma^\mu\} = 0$ was used. Furthermore, the occurrence of the color trace due to the pion being a color singlet was treated in a manner analogous to the color structure of the quark DSE described in App. D.1, which results in a color factor of $\frac{4}{3}$. In consideration of the flavor content of the pion's BSE, it is evident that, under the assumption of isospin symmetry, the flavor matrices on the left and right-hand sides are identical. This follows from the fact that the RL truncated kernel is flavor independent; as a consequence. This allows for the straightforward omission of the flavor content.

It is theoretically possible to project out equations for the dressing functions f_i , however, this approach is not considered to be the most efficient. An alternative method that employs the change of basis into an orthonormal one is considered to be a more effective

²In the chiral limit all current-quark masses vanish

solution and this is the approach taken. To illustrate this, consider the following definition of alternative vectors:

$$d^\mu = \hat{P}^\mu = \frac{P^\mu}{|P|}, \quad r^\mu = \hat{p}_\perp^\mu = \frac{p_\perp^\mu}{|p_\perp|}, \quad p_\perp^\mu = p^\mu - \frac{p \cdot P}{P^2} P^\mu. \quad (4.11)$$

This represents a new basis $\tau_i \in \{\mathbb{1}, \not{d}, \not{r}, \not{r}\not{d}\}$ with the orthonormality relation $\frac{1}{4} \text{tr}(\bar{\tau}_i \tau_j) = \delta_{ij}$. The BSA can be expressed in this basis as

$$\Gamma(P; p) = a_1 \mathbb{1} + a_2 \not{d} + a_3 \not{r} + a_4 \not{r}\not{d}, \quad (4.12)$$

introducing a new set of dressing functions a_i . This formulation is notably simpler to treat numerically than the previous one. The explicit derivation of the equations for the new dressing functions a_i is presented in App. E.1. Due to the pion BSE being homogeneous, it can be solved as an eigenvalue problem. To discuss the structure of this solution strategy, we return to the compact notation of the pion BSE, but with a slight modification.

$$K^{(4)} G_0^{(4)} \Gamma = \lambda(P^2) \Gamma. \quad (4.13)$$

Here an eigenvalue $\lambda(P^2)$ is introduced. The momenta of the pion P is now introduced as an input parameter, and the equations are solved for different values of P^2 until the original equation is recovered by imposing the condition that $\lambda(P^2) = 1$. The resulting pion momentum P thus corresponds to the physical pion mass, $P^2 = -M^2$, denoted as m_π . It is important to cautiously probe the BSE for different P^2 values, as the inputs of the quark propagator are given by $p_\pm^2 = p^2 - \frac{M^2}{4} \pm i M |p| z$. In order to ensure a smooth process, it is necessary that the interior of the parabola in the complex plane spanned by p_\pm^2 is free of poles or cuts in the integrand. However, this is not guaranteed by the quark propagator, which typically has poles. In order to avoid the necessity for more involved methods, such as contour deformation or numerical residue calculation, we restrict P^2 to have a maximal value of $P^2 = -\frac{M^2}{4}$.

The four-dimensional momentum integration was performed numerically using a Gauss-Legendre procedure with 64 grid points for the integration in dq^2 and 16 grid points for the angular integration in dy . The angular integration in dz was performed using a Gauss-Chebyshev procedure of the second kind with 16 grid points. The momentum integration cutoff was set to be

$$\int_0^\infty dq^2 \rightarrow \int_0^{L^2=10^6 \text{ GeV}^2} dq^2. \quad (4.14)$$

The coupled integral equations presented in (E.12) are calculated via fix point iteration until convergence is achieved. As a preliminary step in this iterative process, the a_i values were all set to 1 on the grid. To reconstruct the original set of dressing functions f_i , relations can be derived straightforwardly between the two sets of dressing functions f_i and a_i . With the introduction of s , which serves to enhance readability and is defined as $s = \sqrt{1 - z^2}$, the relations read as

$$\begin{aligned} f_1 &= a_1, & f_2 &= \frac{a_3 z - a_2 s}{m_\pi s}, \\ f_3 &= \frac{-a_3}{m_\pi s z p^2}, & f_4 &= \frac{a_4}{2 i m_\pi s |p|}. \end{aligned} \quad (4.15)$$

Chapter 5

Electromagnetic coupling of quarks

5.1 General remarks

To introduce this section, we consider the coupling of a photon to an onshell spin-1/2 fermion with mass m , as described in [34]. In general, such a coupling is described by the matrix element of the electromagnetic current J^μ . This can be written as

$$J^\mu(k, Q) = i \bar{u}(k_+) \left[F_1(Q^2) \gamma^\mu - \frac{F_2(Q^2)}{2m} \left(-\frac{i}{2} [\gamma^\mu, \gamma^\nu] \right) Q^\nu \right] u(k_-), \quad (5.1)$$

where Q^μ represents the four-momentum of the photon, k_\pm^μ are the outgoing and incoming momenta of the fermion, and $u(k_\pm)$ are the Dirac spinors. Given the onshell nature of the fermion, it follows that $k_\pm^2 = -m^2$. In defining the average momentum k , we set

$$k_\pm = k \pm \frac{Q}{2} \implies k_\pm^2 = k^2 + \frac{Q^2}{4} \pm k \cdot Q = -m^2 \iff \begin{cases} k^2 + \frac{Q^2}{4} = -m^2 \\ k \cdot Q = 0 \end{cases} \quad (5.2)$$

This allows us to fully describe the process by the squared momentum transfer, $Q^2 \geq 0$. Consequently, the electromagnetic structure of the fermion can be identified and described by its Lorentz-invariant form factors, specifically the Dirac form factor $F_1(Q^2)$ and the Pauli form factor $F_2(Q^2)$. This approach has been a successful method for probing the internal structure of hadrons by measuring their form factors.

However, it must be acknowledged that a photon coupling to a hadron will always couple to a quark, and therefore the elementary quantity is the quark-photon vertex, which describes the electromagnetic coupling of quarks to photons and therefore encodes their electromagnetic properties. Nevertheless, it is important to note that an elementary quark is not onshell and does not have a well-defined mass. Consequently, the previously imposed constraints are erased. Notably, there is no longer a necessity for the contraction of onshell spinors on both the left and right sides. Additionally, the constraint that $k_\pm^2 = -m^2$ is no longer valid. As a consequence, the general quark-photon vertex depends on three Lorentz invariants, namely k^2 , Q^2 and $k \cdot Q$. Furthermore, the structure of the Lorentz-Dirac tensor is considerably more intricate. This results in a dependence on 12 tensors, in contrast to the two previously considered form factors, which only contain two tensors. The electromagnetic properties of the quark are now described by 12 dressing functions.

5.2 Quark-Photon vertex

We therefore return to a DSE/BSE formulation of the quark-photon vertex. In order to arrive at the BSE defining the quark-photon vertex, it is necessary to project the two quark and two antiquark four-point Green's function $G^{(4)}$ onto the subspace with the quantum number of the photon¹, as described in [35].

The inhomogeneous BSE thus reads as

$$\Gamma_{qp}^\mu(k, Q) = Z_2 i \gamma^\mu + \int \frac{d^4 k'}{(2\pi)^4} K^{(4)}(Q, k, k') S(k'_+) \Gamma_{qp}^\mu(k', Q) S(k'_-). \quad (5.3)$$

Here, Q represents the photon momentum, k' is the relative momentum of the vertex situated within the momentum loop, $k'_\pm = k' \pm \frac{Q}{2}$ are the quark momenta, and thus $S(k_\pm)$ is the dressed quark propagator. Z_2 is the quark wave function renormalization constant. It should be noted that the appearance of this constant on the bare quark-photon vertex, rather than a separate renormalization constant (denoted by Z_1), is a direct consequence of the Ward-Takahashi identity (WTI), which this vertex must necessarily satisfy due to the conservation of current. The latter identity relates $Z_1 = Z_2$; it can be found in (5.4). It should be noted that the quark-photon vertex $\Gamma_{qp}^\mu(k, Q)$ is a 4×4 - Dirac matrix, with an additional Lorentz index $\mu = 1, \dots, 4$. The interaction kernel $K^{(4)}$, on the other hand, is identical to the kernel employed in the case of the pion BSE, with the result that the kernel is truncated to contain exclusively a gluon exchange among quarks. Consequently, the kernel neglects all electromagnetic corrections to the vertex. The inhomogeneous BSE with the explicit momentum routing is also depicted in Fig. 5.1.

Before we proceed, consider the Ward-Takahashi identity (WTI) on this three-point (vertex) function:

$$S(k_+) [Q_\mu \Gamma_{qp}^\mu(k, Q)] S(k_-) = S(k_-) - S(k_+) \iff Q_\mu \Gamma_{qp}^\mu(k, Q) = S^{-1}(k_+) - S^{-1}(k_-) \quad (5.4)$$

This identity allows us to relate the basis elements longitudinal to the photon momentum Q^μ with the quark propagator $S(k_\pm)$. This motivates a tensor decomposition into longitudinal part² G_i and transverse part T_i respectively

$$\Gamma_{qp}^\mu(k, Q) = \sum_{j=1}^4 g_j^{qp}(k^2, k \cdot Q, Q^2) i G_j^\mu(k, Q) + \sum_{j=1}^8 f_j^{qp}(k^2, k \cdot Q, Q^2) i T_j^\mu(k, Q) \quad (5.5)$$

A basis that is explicitly compatible with the quantum numbers of a photon has been employed on numerous occasions, as evidenced e.g. [35–37]. The basis is as follows:

¹The quantum numbers of a photon are $J^{PC} = 1^{--}$. E.g. under charge conjugation this entails $\bar{\Gamma}_{qp}^\mu(k, Q) = -\Gamma_{qp}^\mu(k, -Q)$.

²The longitudinal part is not precisely longitudinal, although it is often referred to in the literature as such. For example, in the case of vanishing photon momentum ($Q = 0$), the transverse part can also be constrained by the WTI.

$$\begin{aligned}
G_1^\mu &= \gamma^\mu, & T_1^\mu &= t_{QQ}^{\mu\nu} \gamma^\nu, & T_5^\mu &= t_{QQ}^{\mu\nu} i k^\nu, \\
G_2^\mu &= k^\mu \not{k}, & T_2^\mu &= (k \cdot Q) t_{QQ}^{\mu\nu} \frac{i}{2} [\gamma^\nu, \not{k}], & T_6^\mu &= t_{QQ}^{\mu\nu} k^\nu \not{k}, \\
G_3^\mu &= i k^\mu, & T_3^\mu &= \frac{i}{2} [\gamma^\mu, \not{Q}], & T_7^\mu &= (k \cdot Q) t_{Qk}^{\mu\nu} \gamma^\nu, \\
G_4^\mu &= (k \cdot Q) \frac{i}{2} [\gamma^\mu, \not{k}], & T_4^\mu &= \frac{1}{6} [\gamma^\mu, \not{k}, \not{Q}], & T_8^\mu &= t_{Qk}^{\mu\nu} \frac{i}{2} [\gamma^\nu, \not{k}],
\end{aligned}$$

where $t_{ab}^{\mu\nu} = (a \cdot b) \delta^{\mu\nu} - b^\mu a^\nu$ and the triple commutator is defined as $[A, B, C] = [A, B]C + [B, C]A + [C, A]B$.

Consequently, the longitudinal dressing functions g_j^{qp} are completely fixed by the WTI and they read as

$$g_1^{qp} = \frac{A(k_+^2) + A(k_-^2)}{2}, \quad g_2^{qp} = 2 \frac{A(k_+^2) - A(k_-^2)}{k_+^2 - k_-^2}, \quad g_3^{qp} = -2 \frac{B(k_+^2) - B(k_-^2)}{k_+^2 - k_-^2}, \quad g_4^{qp} = 0 \quad (5.6)$$

Furthermore, this allows for a consistency check when solving the inhomogeneous BSE numerically. It can be seen that the vertex up to g_3^{qp} defines the Ball-Chiu vertex [38], which has been commonly used to eliminate the necessity for a numerical treatment of the inhomogeneous BSE. However, this approach has the consequence of losing information, for example, vector meson poles for timelike momenta $Q^2 \leq 0$ are contained in the transverse part. These poles include the ρ -meson and its excitation because it has fitting quantum numbers ($J^{PC} = 1^{--}$).

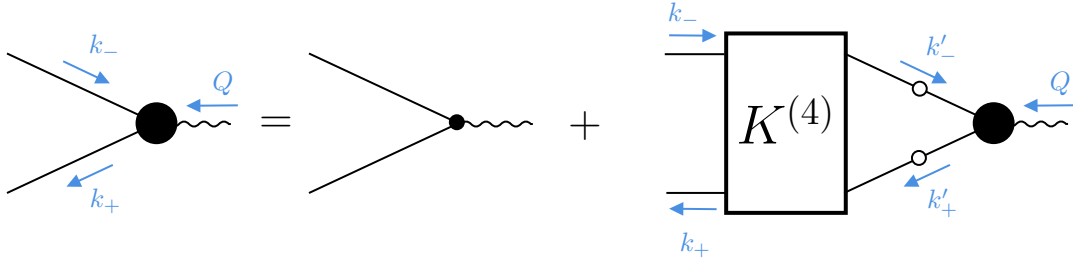


Figure 5.1: Graphical depiction of the inhomogeneous BSE for the quark-photon vertex with explicit momentum routing

At this point, it should be pointed out that the RL truncated kernel $K^{(4)}$ additionally fulfills the vector Ward-Takahashi identity (VWTI)

$$\{\Sigma(k_+) - \Sigma(k_-)\}_{\alpha\beta} = \int K_{\alpha\gamma, \delta\beta}^{(4)}(Q, k, k') \{S(k'_-) - S(k'_+)\}_{\gamma\delta}. \quad (5.7)$$

This is crucial for instance when calculating hadron form factors, as this identity ensures that charge conservation in electromagnetic processes is not violated due to the truncated kernel.

The solution of the inhomogeneous BSE is analogous to that of the pion BSE, with the key distinction being that, due to the inhomogeneity, it is not solved as an eigenvalue

problem. Instead, it is solved for each photon momentum Q via a fixed-point iteration until convergence is reached individually.

The four-dimensional momentum integration was performed numerically using a Gauss-Legendre procedure with 64 grid points for the integration in dq^2 and 16 grid points for the angular integration in dy . The angular integration in dz was performed using a Gauss-Chebyshev procedure of the second kind with 16 grid points. The momentum integration cutoff was set to be

$$\int_0^\infty dq^2 \rightarrow \int_0^{L^2=10^6 \text{ GeV}^2} dq^2. \quad (5.8)$$

For numerical reasons, we switch to a more practical basis, which is orthonormal. NB: This is conceptually analogous to the case for the numerical treatment of the pion BSE.

To shortly sketch this procedure we define a new set of orthonormal vectors as

$$n^\mu = \hat{Q}^\mu = \frac{Q^\mu}{|Q|}, \quad m^\mu = \hat{k}_\perp^\mu = \frac{k_\perp^\mu}{|k_\perp|}, \quad k_\perp^\mu = k^\mu - \frac{k \cdot Q}{Q^2} Q^\mu. \quad (5.9)$$

Together with the definition of the transversely projected γ -matrices as

$$\gamma_\perp^\mu = \gamma^\mu - n^\mu \not{n} - m^\mu \not{m}, \quad (5.10)$$

we arrive at a new orthonormal basis τ_i^{qp} which, fulfils the condition $\frac{1}{4} \text{tr}(\bar{\tau}_i^{qp} \tau_j^{qp}) = \delta_{ij}$. The explicit basis is explicitly stated in (F.3). This introduces a new set of dressing functions, a_j^{qp} with their explicit projected equations derived in the App. F.1.

The relationships between the original set of dressing functions, which include g_j^{qp} and f_j^{qp} , and the a_j^{qp} can be readily established as follows:

$$\begin{aligned} g_1^{qp} &= a_{10}^{qp} - \frac{a_{11}^{qp} z}{s}, & g_2^{qp} &= \frac{a_{11}^{qp}}{k^2 s z}, & g_3^{qp} &= -i \frac{a_9^{qp}}{k z}, & g_4^{qp} &= i \frac{a_{12}^{qp}}{k^2 Q s z}, \\ f_1^{qp} &= \frac{\sqrt{2} a_1^{qp} + 2 s z (a_{11}^{qp} + a_6^{qp}) - 2 z^2 a_7^{qp} - 2 s^2 a_{10}^{qp}}{2 Q^2 s^2}, & f_5^{qp} &= i \frac{a_9^{qp} s - a_5^{qp} z}{k Q^2 z s}, \\ f_2^{qp} &= -i \frac{\sqrt{2} a_2^{qp} z + \sqrt{2} a_3^{qp} s - 2 a_8^{qp} z + 2 a_{12}^{qp} s}{2 k^2 Q^3 z s^2}, & f_6^{qp} &= -\frac{\sqrt{2} a_1^{qp} z - 2 a_7^{qp} z + 2 a_{11}^{qp} s}{2 k^2 Q^2 z s^2}, \\ f_3^{qp} &= i \frac{a_3^{qp} z - a_2^{qp} s}{\sqrt{2} Q s}, & f_7^{qp} &= -\frac{\sqrt{2} a_1^{qp} z + 2 a_6^{qp} s - 2 a_7^{qp} z}{2 k^2 Q^2 z s^2}, \\ f_4^{qp} &= \frac{a_4^{qp}}{\sqrt{2} k Q s}, & f_8^{qp} &= i \frac{\sqrt{2} a_2^{qp} - 2 a_8^{qp}}{2 k^2 Q s^2}, \end{aligned} \quad (5.11)$$

where s is defined as $s = \sqrt{1 - z^2}$.

Chapter 6

Numerical Result

In this chapter, the results of the numerical calculations are presented. The calculations begin with the numerical evaluation of the quark dressing functions, $A(p^2)$ and $M(p^2)$, given by (3.10), where the self-energy terms are projected from the quark DSE and are explicitly available in (D.14) and (D.15). The exponentially scaled modified Bessel functions $\tilde{I}_n(\frac{2pq\eta^2}{\Lambda^2})$ are implemented through an asymptotic expansion provided by [39]. The dressing functions for spacelike momenta ($p^2 > 0$) are depicted in Fig. 6.1.

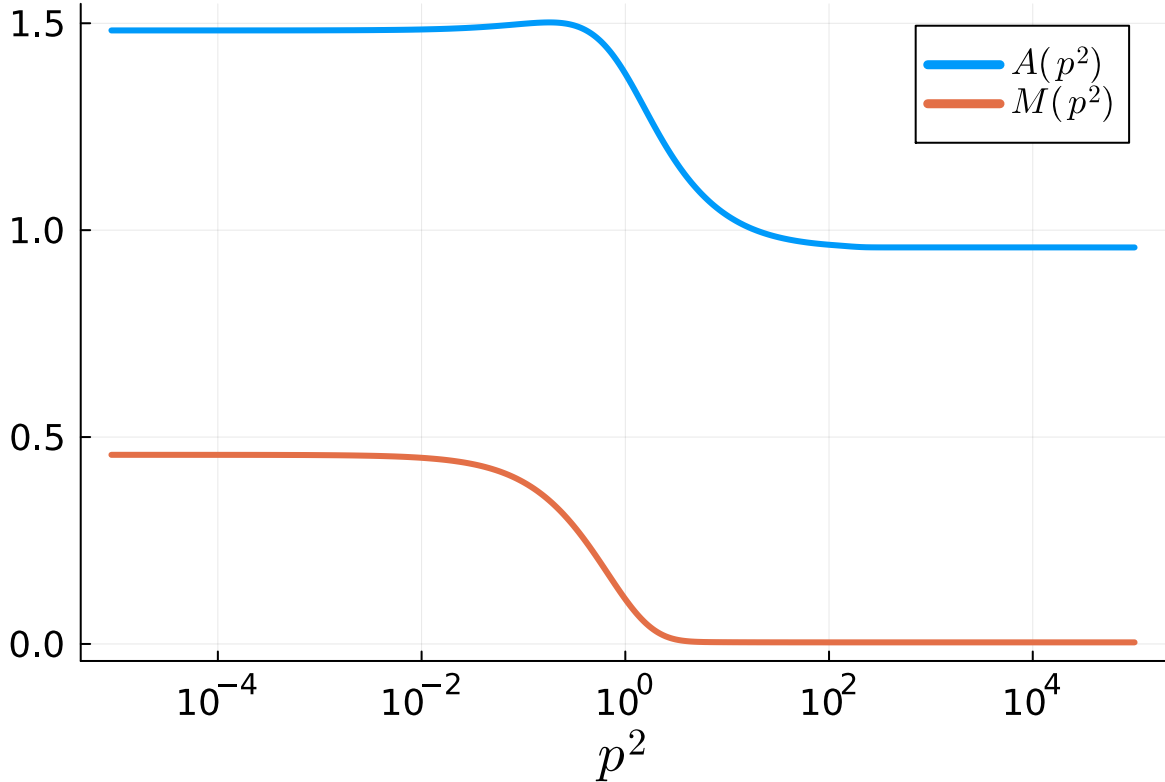


Figure 6.1: Quark dressing functions $A(p^2)$ and $M(p^2)$ with $\eta = 1.8$ and $\Lambda = 0.72$ GeV.

Furthermore the quark renormalization constant Z_2 , was calculated to be $Z_2 = 0.956$.

The quark mass functions exhibit a very notable deviation from the bare quark mass of $m_0 = 4$ MeV. This shows the non-perturbative nature of this approach, where mass is dynamically generated in the infrared sector and is not achievable in any order of a

perturbative calculation. It is essential to attain the highest possible degree of precision in this iterative process for the quark dressing functions, as the converged solution will be used for complex momenta in subsequent calculations.

As mentioned, the quark dressing functions are employed in the calculation of the pion BSA, extracted from the pion BSE. The non-normalized dressing functions of the pion BSA are calculated using (E.12) and (4.15) and are illustrated in Fig. 6.2.

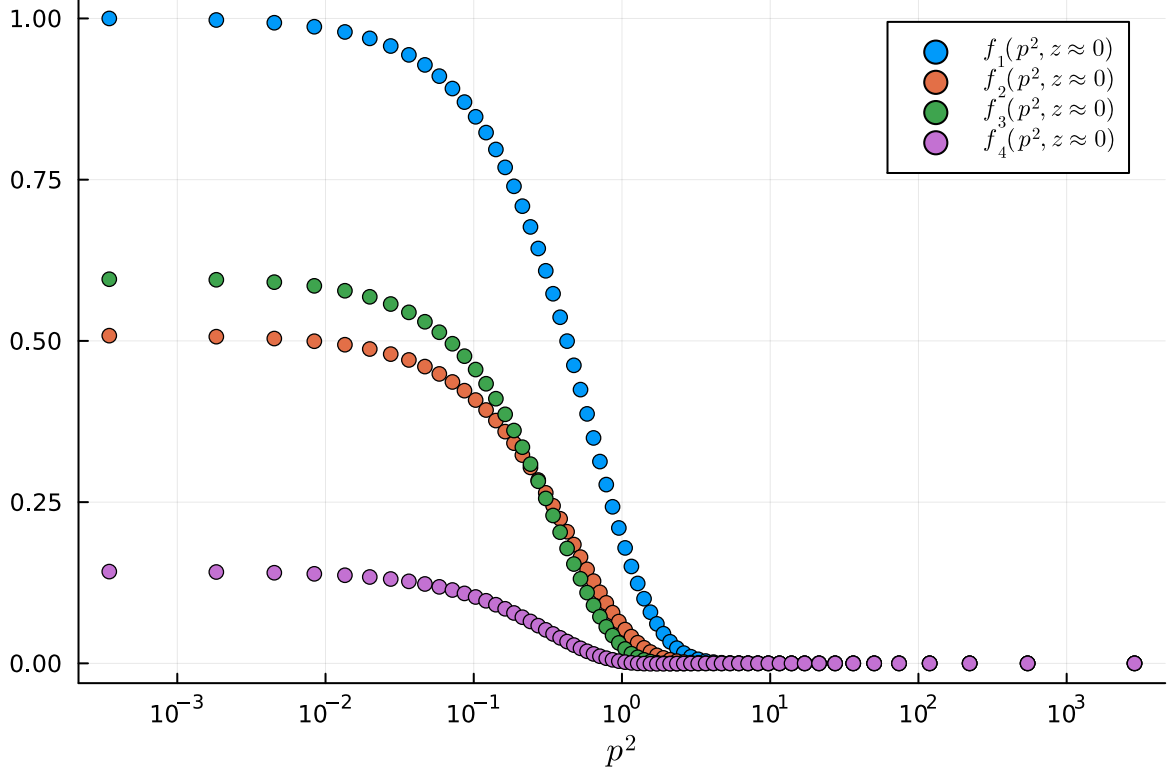


Figure 6.2: The four dressing functions are calculated at $z = 0.092$ (for convenience), but it is irrelevant since the dependence on z is very weak.

As the mass m_π of the pion is an input parameter, the eigenvalue spectrum of the pion BSE is also depicted in Fig. 6.3 and Fig. 6.4. The calculated pion mass, crossing the $\lambda = 1$ line, is $m_\pi = 141.2$ MeV. This result is in excellent agreement with the experimentally measured pion mass of $m_\pi^{exp} = 139.6$ MeV. However, the standard procedure is to fine-tune the parameters η and m_0 such that the pion decay constant f_π is fixed to experiment and all other properties are read off from that set of parameters. As this thesis concerns the qualitative solution of sets of equations such as the pion BSE, the parameter fine-tuning procedure has been omitted.

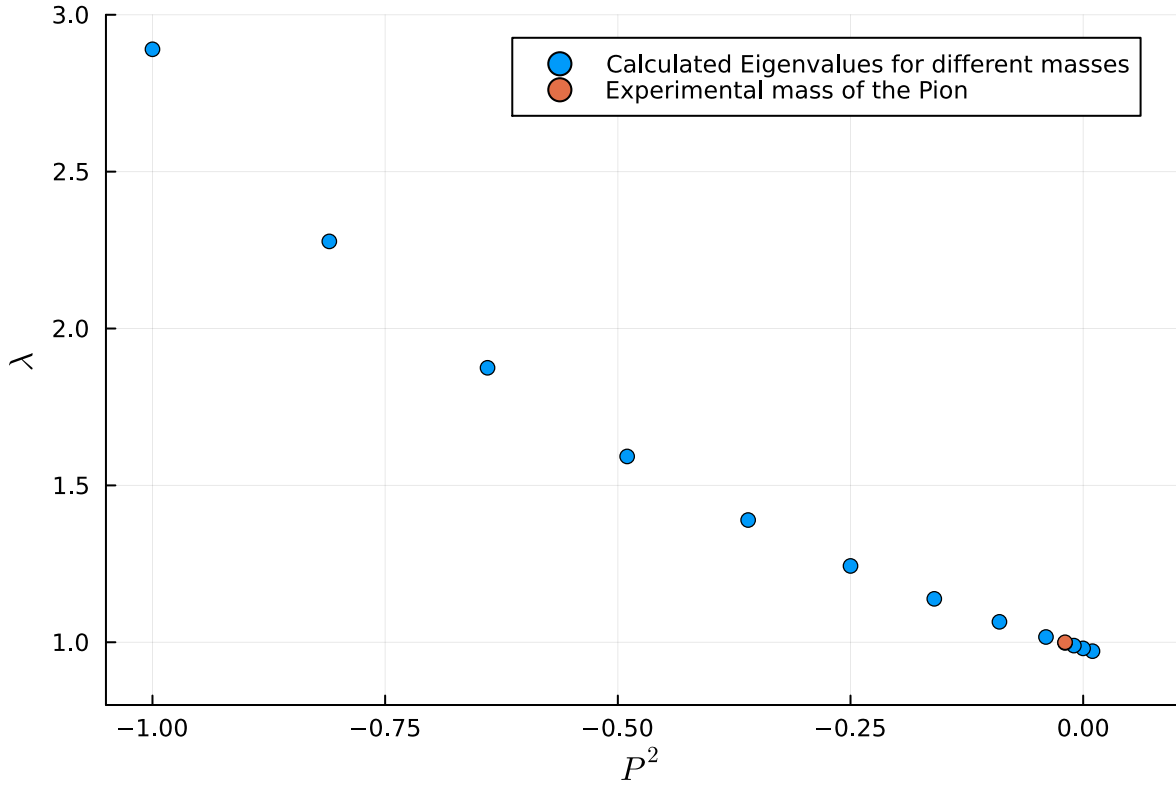


Figure 6.3: Eigenvalue spectrum of the pion BSE.

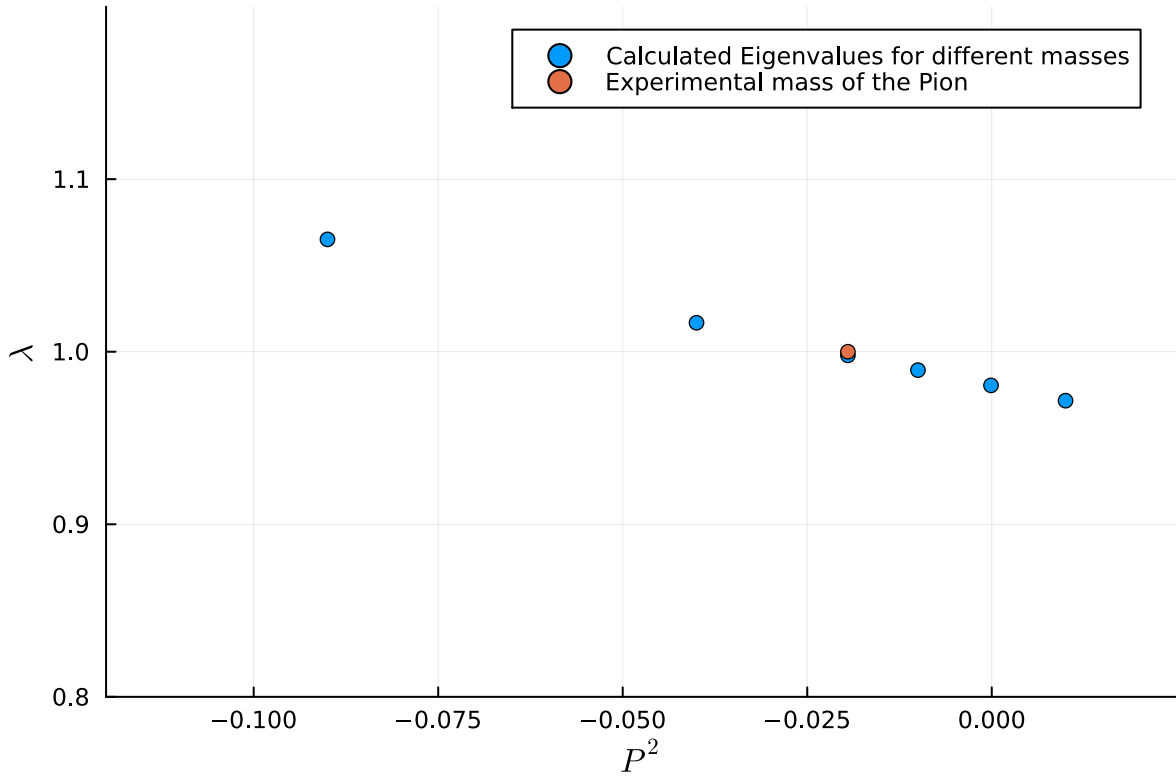


Figure 6.4: zoomed in eigenvalue spectrum of the pion BSE.

The quark-photon vertex dressing functions are calculated using the equations provided in (F.6) and (5.11). The longitudinal dressing functions are depicted in Fig. 6.5. Furthermore, one can verify the accuracy and precision of the calculations by comparing the calculated longitudinal dressing functions, g_1^{qp} , g_2^{qp} , g_3^{qp} and g_4^{qp} , to the exact expressions, which consist of the quark dressing functions, $A(p^2)$ and $M(p^2)$, in (5.6). Thereafter, the transverse dressing functions are depicted in Fig. 6.7 and Fig. 6.8.

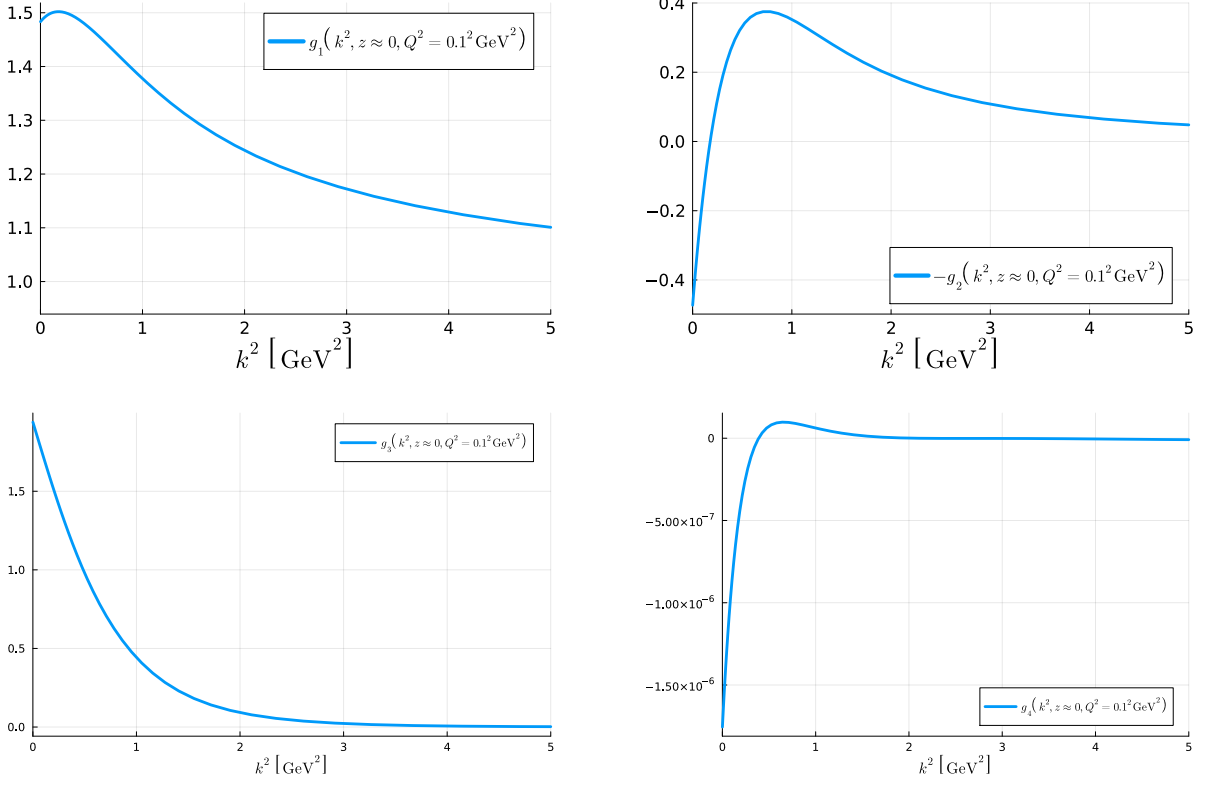


Figure 6.5: The longitudinal dressing functions g_1^{qp} , g_2^{qp} , g_3^{qp} and g_4^{qp} of the quark-photon vertex at $z = 0.092$ and a virtual photon momentum of $Q = 0.1 \text{ GeV}$.

We see here very well that the dressing function g_4^{qp} coincides very well with the solution provided by the WTI $g_4^{qp} = 0$. Consequently, the quark-photon vertex depends on 11 dressing functions. Furthermore, it is worth mentioning that the dressing function g_3^{qp} is related to the quark anomalous magnetic moment¹ (AMM).

¹The quark anomalous magnetic moment describes an observed deviation of the predicted magnetic moment by the Dirac equation for point-like fermions.

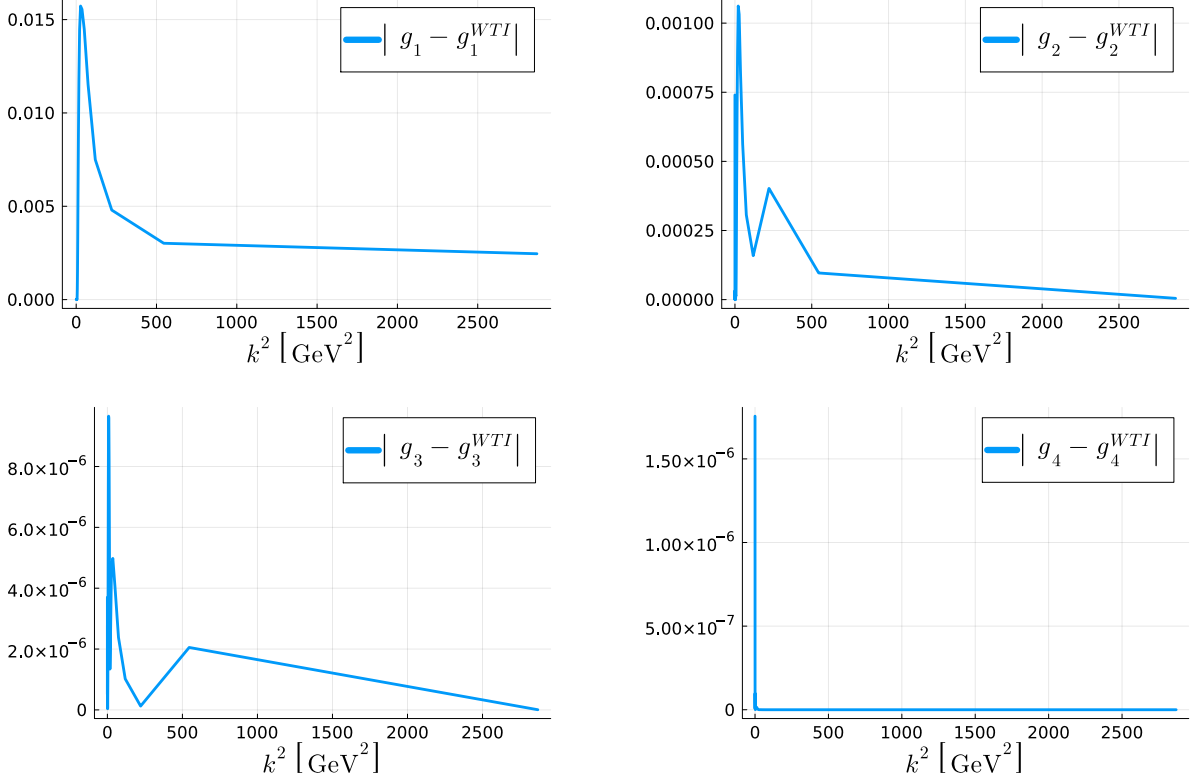


Figure 6.6: The difference between the calculated longitudinal dressing functions g_1 , g_2 , g_3 and g_4 with the exact solution obtained by the WTI g_1^{WTI} , g_2^{WTI} , g_3^{WTI} and g_4^{WTI}

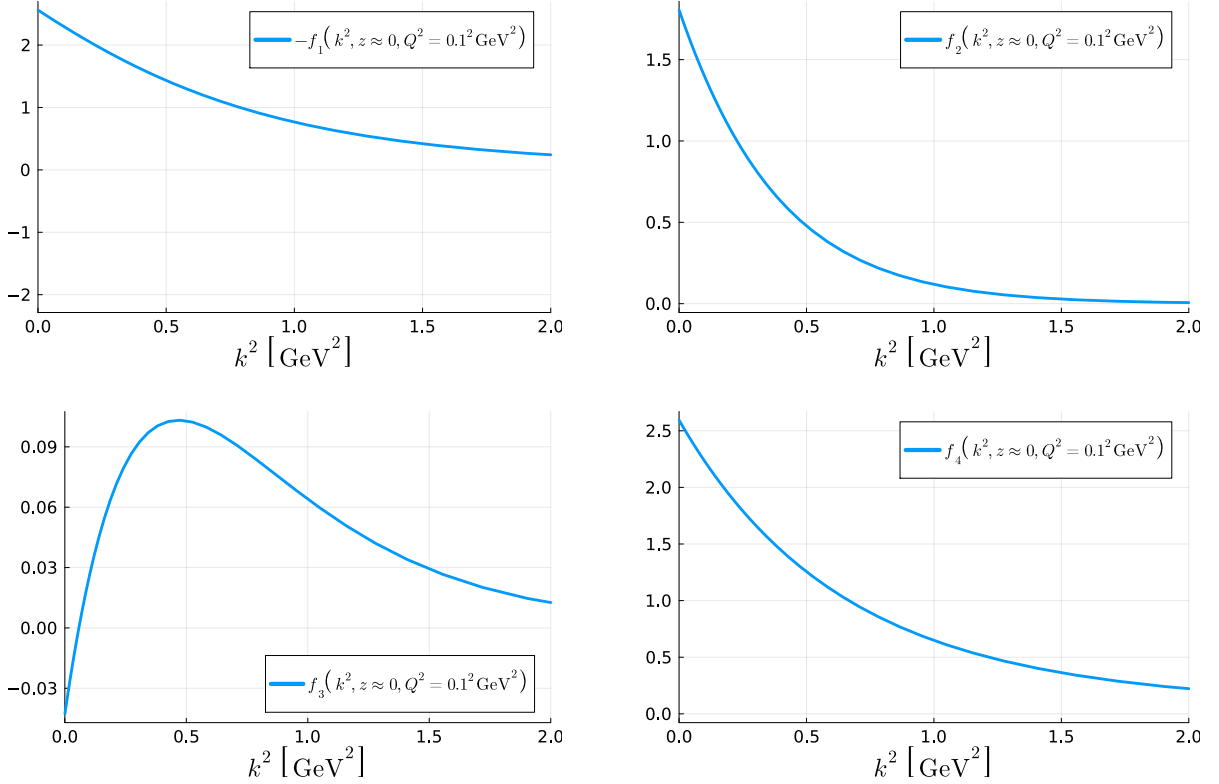


Figure 6.7: The first 4 transverse dressing functions f_1^{qp} , f_2^{qp} , f_3^{qp} and f_4^{qp} of the quark-photon vertex at $z = 0.092$ and a virtual photon momentum of $Q = 0.1$ GeV

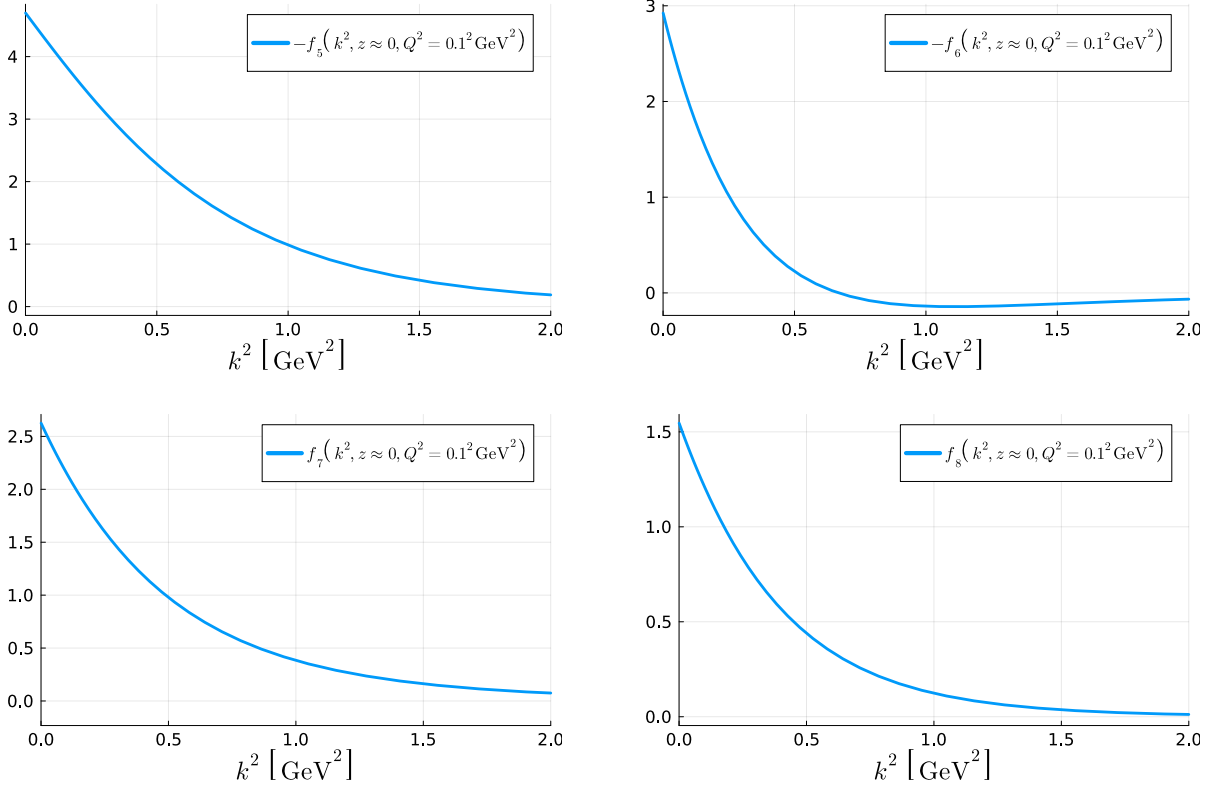


Figure 6.8: The last four transverse dressing functions f_5^{qp} , f_6^{qp} , f_7^{qp} and f_8^{qp} of the quark-photon vertex at $z = 0.092$ and a virtual photon momentum of $Q = 0.1$ GeV

It should be noted that the somewhat obscure choice of evaluating at $z = 0.092$ stems from the fact that the solution is directly taken from the grid on which it was solved. This was the closest point to 0, and while one could interpolate to $z = 0$, this does not affect the qualitative discussion. Furthermore, the plots show the dressing functions for an exemplary virtual photon momentum of $Q = 0.1$ GeV.

The used codes written in the programming language *Julia* and the *Mathematica* files are available in the GitHub repository <https://github.com/IGrozav/GrozavBATHesis>.

Chapter 7

Summary

A rainbow ladder truncated BSE/DSE approach was employed in conjunction with a simplified version of the Maris-Tandy model cf. (3.8) instead of the full Maris-Tandy model (C.2) to derive and solve the

- Quark DSE,
- Pion BSE,
- Quark-photon vertex BSE.

The quark-photon vertex has been calculated for the first time for that employed model. The choice of rainbow ladder truncated quark-antiquark interaction allowed for the preservation of:

- The chiral symmetry and its dynamical breaking, which leads to massless pions for vanishing bare quark masses and the confinement of quarks and gluons in hadrons, are also exhibited.
- The charge conservation, which is crucial for a correct calculation of hadronic form factors, is also exhibited. This is in accordance with the VWTI.

The non-perturbative nature is exhibited for instance in the quark mass function $M(p^2)$, where mass is dynamically generated in the infrared sector.

The numerical calculation of the longitudinal dressing functions of the quark-photon vertex exhibits a deviation of a smaller percentile except for small momenta, where the error is of order $\mathcal{O}(1\%)$ from the exact solution, which are fixed by the WTI. This allows us to conclude that the numeric implementation is accurate. Furthermore, we expect to observe the vector meson poles, which lie in the timelike region of $k^2 < 0$ in all eight transverse dressing functions. These are indicated by rising values as k^2 approaches zero. This demonstrates that the BC Ansatz for the quark-photon vertex is not sufficient for a form factor calculation.

Finally, we have included a comprehensive appendix containing all explicit expressions and conventions used.

Acknowledgements

I would like to express my gratitude to Professor G. Eichmann for his valuable insights and contributions during our discussion regarding the Pion BSE. His assistance was invaluable in deriving the explicit expression presented in the attached appendix [D](#), [E](#) and [F](#).

Appendix A

Conventions

A.1 Euclidean field theory

Quantum field theory is formulated in physical Minkowski spacetime. An analytical continuation for the time component leads to an Euclidean spacetime. The main motivation behind this mathematical trick, called *Wick rotation* is that practical calculations are often simpler in Euclidean spacetime. Explicitly, the Minkowski spacetime volume becomes after defining $x_4 = ix_0$,

$$i \int d^4 x_M = i \int d^3 x \int_{-\infty(1-i\epsilon)}^{\infty(1-i\epsilon)} x_4 \stackrel{x_4 = ix_0}{=} \int d^3 x \int_{-\infty}^{\infty} dx_4 := \int d^4 x_E. \quad (\text{A.1})$$

Recall the importance of the $i\epsilon$ prescription in the time limits, which makes the integration path slightly below and above the real axis to preserve causality, and makes Green functions well-defined objects in quantum field theory. This motivates an Euclidean four-vector x_E^μ as

$$\begin{aligned} x_E^\mu &= \begin{pmatrix} \mathbf{x} \\ ix_0 \end{pmatrix} \implies x_E^2 = x_E^\mu \delta_{\mu\nu} x_E^\nu = \mathbf{x}^2 - x_0^2, \\ x_M^\mu &= \begin{pmatrix} x_0 \\ \mathbf{x} \end{pmatrix} \implies x_M^2 = x_M^\mu \eta_{\mu\nu} x_M^\nu = x_0^2 - \mathbf{x}^2 = -x_E^2, \end{aligned} \quad (\text{A.2})$$

where $\delta_{\mu\nu}$ represents the Euclidean metric tensor and $\eta_{\mu\nu}$ the Minkowski metric tensor with signature $(+, -, -, -)$. This relates the Euclidean scalar product to the Minkowski scalar product as $x_E^2 = -x_M^2$, or more generally, that the Lorentz invariant scalar product of any two four-vectors differs by a minus sign in the Euclidean convention from its Minkowski counterpart

$$(a \cdot b)_E = -(a \cdot b)_M. \quad (\text{A.3})$$

Upon applying the replacement rule above on the γ -matrices defined as $\gamma_M^\mu = (\gamma_0, \boldsymbol{\gamma})^T \rightarrow \gamma_E^\mu = (\boldsymbol{\gamma}, i\gamma_0)^T$, one observes some inconveniences. For instance, the Clifford algebra changes the sign: $\{\gamma_E^\mu, \gamma_E^\nu\} = -2\delta^{\mu\nu}$. This motivates a redefinition of the γ -matrices as $\gamma_E^\mu \rightarrow \tilde{\gamma}_E^\mu = -i\gamma_E^\mu$, which results in

$$\begin{aligned} \gamma_E^\mu &= \begin{pmatrix} -i\boldsymbol{\gamma} \\ \gamma_0 \end{pmatrix}, \quad \not{x}_E = i\not{x}_M, \quad \{\gamma_E^\mu, \gamma_E^\nu\} = 2\delta^{\mu\nu}, \\ \gamma_E^5 &= -(\gamma^1 \gamma^2 \gamma^3 \gamma^0)_E = i(\gamma^0 \gamma^1 \gamma^2 \gamma^3)_M = \gamma_M^5. \end{aligned} \quad (\text{A.4})$$

Hence, in the framework of Euclidean field theory, we rename $\gamma^0 \rightarrow \gamma^4$ to obtain $\gamma_E^5 = -(\gamma_1 \gamma_2 \gamma_3 \gamma_4)_E$.

In standard representation the Euclidean space γ_E^μ matrices read as:

$$\gamma_E^j = \begin{pmatrix} 0 & -i\tau_j \\ i\tau_j & 0 \end{pmatrix}, \quad \gamma_E^4 = \begin{pmatrix} \mathbb{1}_2 & 0 \\ 0 & -\mathbb{1}_2 \end{pmatrix}, \quad \gamma_E^5 = \begin{pmatrix} 0 & \mathbb{1}_2 \\ \mathbb{1}_2 & 0 \end{pmatrix}, \quad (\text{A.5})$$

where $\mathbb{1}_2$ reads as the 2×2 identity matrix and τ_j are the standard Pauli matrices given as

$$\tau_1 = \begin{pmatrix} 0 & 1 \\ 1 & 0 \end{pmatrix}, \quad \tau_2 = \begin{pmatrix} 0 & -i \\ i & 0 \end{pmatrix}, \quad \tau_3 = \begin{pmatrix} 1 & 0 \\ 0 & -1 \end{pmatrix}. \quad (\text{A.6})$$

Additionally, the four-vector derivative transforms due to (A.2) in the following way

$$\partial_\mu^M = \begin{pmatrix} \partial_0 \\ \nabla \end{pmatrix} \rightarrow \partial_\mu^E = \begin{pmatrix} \nabla \\ -i\partial_0 \end{pmatrix}, \quad (\text{A.7})$$

which implies that $(\partial \cdot a)_M = (\partial \cdot a)_E$.

The gauge invariant QCD action in the physical Minkowski space transforms to Euclidean space therefore as:

$$\begin{aligned} e^{iS_M} &= \exp \left[i \int d^4x \left(\sum_f \bar{q}^{(f)} \left(i \not{D}^M - m^{(f)} \right) q^{(f)} - \frac{1}{2} \text{tr}_c [F_{\mu\nu}^M F_{\mu\nu}^M] \right) \right] = \\ &= \exp \left[- \int d^4x \left(\sum_f \bar{q}^{(f)} \left(\not{D}^E + m^{(f)} \right) q^{(f)} + \frac{1}{2} \text{tr}_c [F_{\mu\nu}^E F_{\mu\nu}^E] \right) \right] := e^{-S_E}, \end{aligned} \quad (\text{A.8})$$

where $D_\mu^M = \partial_\mu^M - igA_\mu^M$, $D_\mu^E = \partial_\mu^E + igA_\mu^E$ and $(F_{\mu\nu} F^{\mu\nu})_M = (F_{\mu\nu} F_{\mu\nu})_E$.

This thesis is formulated with the Euclidean convention. The index E will be therefore always implicit.

A.2 Integration over Hyperspherical coordinates

Hyperspherical coordinates are a generalization of the spherical coordinates in higher dimensions as 3. Expressing a four-vector q^μ in these coordinates takes generally the following form:

$$q^\mu = |q| \begin{pmatrix} \sin \theta_2 \sin \theta_1 \sin \phi \\ \sin \theta_2 \sin \theta_1 \cos \phi \\ \sin \theta_2 \cos \theta_1 \\ \cos \theta_2 \end{pmatrix}^\mu \quad (\text{A.9})$$

with the four-dimensional integral measure

$$d^4q = dq |q|^3 d\theta_1 \sin \theta_1 d\theta_2 \sin^2 \theta_2 d\phi, \quad (\text{A.10})$$

$$q \in [0, \infty], \quad \theta_1 \in [0, \pi], \quad \theta_2 \in [0, \pi], \quad \phi \in [0, 2\pi).$$

We first employ the following substitution

$$\cos(\theta_1) = y \rightarrow d\theta_1 \sin \theta_1 = -dy, \quad \cos(\theta_2) = z \rightarrow d\theta_2 \sin^2 \theta_2 = -\sqrt{1-z^2} dz.$$

In addition with $dq|q|^3 = \frac{1}{2}dq^2q^2$ to end up with

$$q^\mu = |q| \begin{pmatrix} \sqrt{1-z^2} \sqrt{1-y^2} \sin \phi \\ \sqrt{1-z^2} \sqrt{1-y^2} \cos \phi \\ \sqrt{1-z^2} y \\ z \end{pmatrix}^\mu \quad (\text{A.11})$$

with the four-dimensional integral measure

$$d^4q = \frac{1}{2} dq^2 q^2 dz \sqrt{1-z^2} dy d\phi, \quad (\text{A.12})$$

$$q \in [0, \infty], \quad z \in [-1, 1], \quad y \in [-1, 1], \quad \phi \in [0, 2\pi).$$

Appendix B

QCD Feynman rules

The Feynman rules are a helpful tool for reconstructing the equations of a given Feynman diagram. These rules are determined solely by the underlying Lagrangian. As this thesis requires the use of the quark propagator, gluon propagator, and quark-gluon vertex, only these objects will be mentioned and are a collection from [40].

B.1 Renormalized QCD Feynman rules

For the renormalized version of the QCD Lagrangian in (2.2) we replace the following quantities in the QCD Lagrangian by their renormalized quantities

$$q \rightarrow Z_2^{1/2} q, \quad A \rightarrow Z_3^{1/2} A, \quad c \rightarrow \tilde{Z}_3^{1/2} c, \quad m \rightarrow Z_m m, \quad g \rightarrow Z_g g. \quad (\text{B.1})$$

Bare quantities will have a 0 as an index, e.g. m_0 for the bare quark mass. The renormalized quantities enter therefore in the Feynman rules.

In the following, it is demonstrated that the propagators are diagonal in color space, which is expressed as a factor of δ_{ij} . The quark-gluon vertices exhibit some color structure, where the t_a represents the a^{th} generator of $\text{SU}(3)_c$ and i, j are the color indices with respect to the fundamental representation.

B.1.1 Quark Propagator

The tree-level quark propagator can be read as

$$\alpha, i \xrightarrow[p]{\longleftarrow} \beta, j \quad S_0(p)^{-1} = Z_2 (i\not{p} + m_0) \delta_{ij} \iff S_0(p) = \frac{1}{Z_2} \frac{-i\not{p} + m_0}{p^2 + m_0^2} \delta_{ij}. \quad (\text{B.2})$$

Going beyond the tree-level propagator, we can expand the full quark propagator $S(p)$ into an appropriate Lorentz-covariant tensor basis

$$S(p) = \sum_i f_i(p^2) \tau_i(p). \quad (\text{B.3})$$

Since the quark propagator depends only on one momentum p , we conclude that the only possible tensor structures are $\tau \in \{\mathbb{1}, \not{p}\}$. Following the nomenclature of the literature we

obtain the Feynman rule for the full (or dressed) quark propagator as

Diagram illustrating a vertex with two external legs. The left leg is labeled α, i and the right leg is labeled β, j . A momentum p is shown entering the vertex from the right, with a minus sign -1 next to it.

$$S^{-1}(p) = A(p^2)(i\not{p} + M(p^2)) \delta_{ij} \iff S(p) = \frac{1}{A(p^2)} \frac{-i\not{p} + M(p^2)}{p^2 + M^2(p^2)} \delta_{ij}. \quad (\text{B.4})$$

Herein the dressing function $M(p^2)$ is called the *quark mass function* and $\frac{1}{A(p^2)}$ is called the *quark wave-function renormalization*

B.1.2 Gluon Propagator

The Feynman rule for the tree-level gluon propagator is

$$\begin{aligned}
& \mu, a \overset{\overleftarrow{q}}{\text{---}\!\!\!\!\!\! \sim\!\!\!\!\!\! \text{---}}^{-1} \nu, b \\
(D_0^{\mu\nu})^{-1}(q) &= q^2 \left[Z_3 \left(\delta^{\mu\nu} - \frac{q^\mu q^\nu}{q^2} \right) + \frac{1}{\xi} \frac{q^\mu q^\nu}{q^2} \right] \delta_{ab} \iff \\
D_0^{\mu\nu}(q) &= \frac{1}{q^2} \left[Z_3 \left(\delta^{\mu\nu} - \frac{q^\mu q^\nu}{q^2} \right) + \xi \frac{q^\mu q^\nu}{q^2} \right] \delta_{ab}.
\end{aligned} \tag{B.5}$$

This equation consists of a transverse and a longitudinal part, which defines the transverse projector as $T_q^{\mu\nu} = \delta^{\mu\nu} - \frac{q^\mu q^\nu}{q^2}$ and the longitudinal projector as $L_q^{\mu\nu} = \frac{q^\mu q^\nu}{q^2}$. Here it becomes apparent why we choose to work in Landau gauge ($\xi = 0$) \rightarrow the longitudinal part vanishes.


For the full (or dressed) gluon propagator we obtain

$$\begin{aligned}
 & \mu, a \text{ --- } \textcircled{\hspace{-0.8cm}}^q_{\leftarrow -1} \nu, b \\
 (D^{\mu\nu})^{-1}(q) = q^2 \left[Z(q^2) \left(\delta^{\mu\nu} - \frac{q^\mu q^\nu}{q^2} \right) + \frac{1}{\xi} \frac{q^\mu q^\nu}{q^2} \right] \delta_{ab} &\iff \\
 D^{\mu\nu}(q) = \frac{1}{q^2} \left[Z(q^2) \left(\delta^{\mu\nu} - \frac{q^\mu q^\nu}{q^2} \right) + \xi \frac{q^\mu q^\nu}{q^2} \right] \delta_{ab}.
 \end{aligned}
 \tag{B.6}$$

Due to Slavnov-Taylor identities only the transverse part picks up a dressing function $Z(q^2)$.

B.1.3 Quark-Gluon vertex

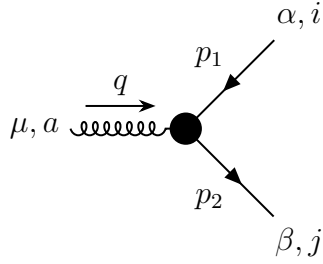
The Feynman rule for the bare quark-gluon vertex is



A Feynman diagram showing a vertex (black dot) with a wavy line entering from the left, labeled with momentum q and indices μ, a . Two straight lines exit the vertex to the right: the upper one is labeled with momentum p_1 and indices α, i , and the lower one is labeled with momentum p_2 and indices β, j .

$$\Gamma_0^\mu = i g (t_a)_{ij} Z_{1f} \gamma^\mu, \quad Z_{1f} = Z_g Z_3^{1/2} Z_2. \quad (\text{B.7})$$

We define the relative gluon momentum $p = \frac{p_1+p_2}{2}$. The full quark-gluon vertex becomes rather involved because there are 4 independent four-vectors and four types of scalars, which allow for 12 possible tensor structures $\tau \in \{\gamma^\mu, p^\mu, q^\mu\} \otimes \{\mathbb{1}, \not{p}, \not{q}, [\not{p}, \not{q}]\}$ [41] :



$$\Gamma^\mu(p, q) = i g (t_a)_{ij} \sum_{k=1}^{12} f_k(p^2, q^2, p \cdot q) \tau_k^\mu(p, q). \quad (\text{B.8})$$

Appendix C

Truncation scheme

C.1 Rainbow-ladder truncation

The underlying concept is based on the substitution of the full quark-gluon vertex by a simplified one. The approach described here allows the quark to emit and then absorb a single gluon. In other words, both the vertex at which the gluon is emitted and the vertex at which it is absorbed are both represented as a bare vertex. The ansatz defining the rainbow-ladder (RL) truncation is given by

$$\Gamma^\mu(l, k) = f(k^2) i\gamma^\mu. \quad (\text{C.1})$$

This equation simplifies the full quark-gluon vertex, which consists of 12 possible tensor structures, to only the first term. While alternative simpler truncation schemes exist, the RL truncation is superior due to its consistency with chiral symmetry, which preserves the Goldstone nature of the pion [31].

C.2 Maris-Tandy model for the effective interaction

In order to ensure the free propagation of emitted gluons while simultaneously simplifying the gluon propagator, this approach is complemented with an effective interaction. This interaction takes into consideration the dressed gluon propagator dressing function, $Z(k^2)$, which enters the RL truncated quark-gluon vertex with its dressing function, $f(k^2)$. The resulting expression is in the Maris-Tandy model expressed as follows:

$$\alpha(k^2) = \frac{g^2}{4\pi} \frac{Z_{1f}}{Z_2^2} Z(k^2) f(k^2) = \pi\eta^7 \left(\frac{k^2}{\Lambda^2} \right)^2 e^{-\eta \frac{k^2}{\Lambda^2}} + \frac{2\pi\gamma_m \left(1 - e^{-\frac{k^2}{\Lambda_t^2}} \right)}{\ln \left(e^2 - 1 + \left(1 + \frac{k^2}{\Lambda_{QCD}^2} \right)^2 \right)}. \quad (\text{C.2})$$

The first term is the infrared sector (small momenta), which encodes the non-perturbative physics with typical values for the parameters of $\Lambda = 0.72 \text{ GeV}$ and $1.6 \leq \eta \leq 2.0$. Throughout this thesis, a value of $\eta = 1.8$ was chosen. The second term account for the correct perturbative behavior at large momenta with the parameters $\Lambda_t = 1 \text{ GeV}$, $\Lambda_{QCD} = 0.234 \text{ GeV}$ and $\gamma_m = \frac{12}{25}$.

The name is derived from the fact that, following the application of the truncation scheme, the remaining Feynman diagrams in the quark DSE resemble rainbows due to the successive emission and absorption of one gluon. The truncation scheme is also employed in the pion BSE, resulting in an interaction kernel that resembles a ladder of transferred gluons.

It should be noted that the k^4 factor in the infrared sector of equation (C.2) is only for technical convenience. This factor cancels out a $\frac{1}{k^2}$ in the gluon propagator that enters the quark DSE. Additionally, this factor cancels the kinematic singularity from the transverse projector $T_k^{\mu\nu}$, allowing for a straightforward calculation of the quark propagator in the entire complex plane, as discussed in [22].

Appendix D

Further information to the Quark DSE

D.1 Color structure of the quark DSE

The color contribution of the quark DSE in (3.3) is straightforward, as the left-hand side of the equation is simply the inverse dressed quark propagator, which is diagonal in color space. The same is true for the bare inverse quark propagator on the right-hand side. A similar argument can be made for the bare inverse quark propagator on the right-hand side. With regard to the self-energy term, we simply adhere to the prescription set out in the Feynman rules in the App. B.1, which ultimately leads to the result

$$\begin{aligned} C_F &= \delta_{jk} \delta^{ab} (t_a)_{ij} (t_b)_{kl} \\ &= (t_a)_{ik} (t_a)_{jl} \\ &= \frac{1}{2} (\delta_{il} \delta_{jj} - \frac{1}{N_C} \delta_{ik} \delta_{jl}) \\ &= \frac{1}{2} (N_C - \frac{1}{N_C}) \delta_{il} \\ &= \frac{N_C^2 - 1}{2N_C} \delta_{il} \\ &\stackrel{N_C=3}{=} \frac{4}{3} \delta_{il}. \end{aligned} \tag{D.1}$$

This can be interpreted as a prefactor to the self-energy term, given that the left- and right-hand sides of the equation are proportional to δ_{il} . It should be noted that from the second to the third line of equation (D.1), the Fierz identity has been employed.

D.2 Dirac structure of the quark DSE

Our work is conducted within the rest frame of the quark, which implies that

$$p^\mu = |p| \begin{pmatrix} 0 \\ 0 \\ 0 \\ 1 \end{pmatrix}^\mu. \tag{D.2}$$

Furthermore, the integration over the variables y and ϕ is trivial, allowing us to work equivalently with the vector

$$q^\mu = |q| \begin{pmatrix} 0 \\ 0 \\ \sqrt{1-z^2} \\ z \end{pmatrix}^\mu \quad (\text{D.3})$$

for the internal momentum. The gluon momentum is then

$$k^\mu = q^\mu - p^\mu \iff k^2 = p^2 + q^2 - 2pqz. \quad (\text{D.4})$$

With this established, we recall the explicit expression of the self-energy term

$$\Sigma(p) = \frac{16\pi}{3} Z_2^2 \int \frac{d^4 q}{(2\pi)^4} \frac{\alpha(k^2)}{k^2} T_k^{\mu\nu} \gamma^\mu \frac{1}{A(q^2)} \frac{-i\not{q} + M(q^2)}{q^2 + M(q^2)^2} \gamma^\nu, \quad (\text{D.5})$$

which leads to the explicit equation for the dressing function $\Sigma_A(p^2) = -\frac{1}{4p^2} \text{tr}(i\not{p} \Sigma(p^2))$

$$\Sigma_A(p^2) = \frac{16\pi}{3} Z_2^2 \int \frac{d^4 q}{(2\pi)^4} \frac{\alpha(k^2)}{k^2} \frac{1}{A(q^2)} \frac{1}{q^2 + M(q^2)^2} \frac{1}{4p^2} \text{tr}(-i\not{p} \gamma^\mu (-i\not{q} + M(q^2)) \gamma^\nu T_k^{\mu\nu}) \quad (\text{D.6})$$

We now focus on the trace only. In this case, the term proportional to $M(q^2)$ vanishes, as we have an odd number of γ -matrices. The only term remaining is

$$\begin{aligned} \text{tr}((-i\not{p}) \gamma^\mu (-i\not{q}) \gamma^\nu T_k^{\mu\nu}) &= 4p \cdot q + \frac{8}{k^2} (p \cdot k)(q \cdot k) \\ &= 12p \cdot q - \frac{8}{k^2} (p^2 q^2 - (p \cdot q)^2) \\ &= 12pqz + (z^2 - 1) \frac{8p^2 q^2}{k^2}. \end{aligned} \quad (\text{D.7})$$

Consequently, the equation becomes then

$$\Sigma_A(p^2) = \frac{16\pi}{3} Z_2^2 \int \frac{d^4 q}{(2\pi)^4} \frac{1}{A(q^2)} \frac{1}{q^2 + M(q^2)^2} \frac{\alpha(k^2)}{k^2} \left[\frac{3qz}{p} - \frac{2q^2}{k^2} (1 - z^2) \right]. \quad (\text{D.8})$$

For the 2nd dressing function $\Sigma_M(p^2) = \frac{1}{4} \text{tr}(\Sigma(p^2))$ we obtain

$$\Sigma_M(p^2) = \frac{16\pi}{3} Z_2^2 \int \frac{d^4 q}{(2\pi)^4} \frac{\alpha(k^2)}{k^2} \frac{1}{A(q^2)} \frac{1}{q^2 + M(q^2)^2} \frac{1}{4} \text{tr}(\gamma^\mu (-i\not{q} + M(q^2)) \gamma^\nu T_k^{\mu\nu}) \quad (\text{D.9})$$

In this case, only the term proportional to $M(q^2)$ remains

$$\begin{aligned} \text{tr}(\gamma^\mu \gamma^\nu T_k^{\mu\nu}) &= \text{tr}(\gamma^\mu \gamma^\mu) - \text{tr}\left(\frac{(\not{p} - \not{q})^2}{(p - q)^2}\right) \\ &= 16 - 4 \\ &= 12. \end{aligned} \quad (\text{D.10})$$

The explicit equation becomes then

$$\Sigma_M(p^2) = 16\pi Z_2^2 \int \frac{d^4 q}{(2\pi)^4} \frac{\alpha(k^2)}{k^2} \frac{1}{A(q^2)} \frac{M(q^2)}{q^2 + M(q^2)^2}. \quad (\text{D.11})$$

D.3 Analytical angular integration

In order to use the quark propagator accurately in the complex plane we must solve it with high precision on the real axis. To achieve that we noticed that the integration over the angular variable z in (D.8) and (D.11) can be done analytically, due to neglecting the $\alpha_{UV}(k^2)$ term in the effective interaction $\alpha(k^2)$. Only the relevant part for this integration is regarded:

$$\begin{aligned} & \int_{-1}^1 dz \sqrt{1-z^2} k^2 e^{-\eta \frac{k^2}{\Lambda^2}} \left(\frac{3qz}{p} + (z^2 - 1) \frac{2q^2}{k^2} \right) = \\ & = \frac{3\pi \Lambda^2}{2p^2 \eta^4} e^{-(p-q)^2 \frac{\eta^2}{\Lambda^2}} \left[-2pq\eta^2 \tilde{I}_1 \left(\frac{2pq\eta^2}{\Lambda^2} \right) + (2\Lambda^2 + (p^2 + q^2) \eta^2) \tilde{I}_2 \left(\frac{2pq\eta^2}{\Lambda^2} \right) \right] \end{aligned} \quad (D.12)$$

$$\begin{aligned} & \int_{-1}^1 dz \sqrt{1-z^2} k^2 e^{-\eta \frac{k^2}{\Lambda^2}} = \\ & = \frac{\pi \Lambda^2}{2pq\eta^2} e^{-(p-q)^2 \frac{\eta^2}{\Lambda^2}} \left[(p^2 + q^2) \tilde{I}_1 \left(\frac{2pq\eta^2}{\Lambda^2} \right) - 2pq \tilde{I}_2 \left(\frac{2pq\eta^2}{\Lambda^2} \right) \right] \end{aligned} \quad (D.13)$$

In this expressions $\tilde{I}_n(x)$ denotes exponentially rescaled modified Bessel functions and are connected to regular modified Bessel functions via $\tilde{I}_n(x) = e^{-|x|} I_n(x)$.

D.4 Explicit expressions for the self energy dressing functions

The explicit expression for the quark dressing function becomes:

$$\begin{aligned} \Sigma_A(p^2) &= \frac{\eta^3}{\Lambda^2} \frac{Z_2^2}{p^2} \int dq^2 \frac{q^2}{A(q^2)} \frac{1}{q^2 + M(q^2)^2} e^{-(p-q)^2 \frac{\eta^2}{\Lambda^2}} \\ &\quad \times \left[-2pq\eta^2 \tilde{I}_1 \left(\frac{2pq\eta^2}{\Lambda^2} \right) + (2\Lambda^2 + (p^2 + q^2) \eta^2) \tilde{I}_2 \left(\frac{2pq\eta^2}{\Lambda^2} \right) \right] \end{aligned} \quad (D.14)$$

$$\begin{aligned} \Sigma_M(p^2) &= \frac{\eta^5}{\Lambda^2} \frac{Z_2^2}{p} \int dq^2 \frac{q}{A(q^2)} \frac{M(q^2)}{q^2 + M(q^2)^2} e^{-(p-q)^2 \frac{\eta^2}{\Lambda^2}} \\ &\quad \times \left[(p^2 + q^2) \tilde{I}_1 \left(\frac{2pq\eta^2}{\Lambda^2} \right) - 2pq \tilde{I}_2 \left(\frac{2pq\eta^2}{\Lambda^2} \right) \right] \end{aligned} \quad (D.15)$$

Appendix E

Further information to the Pion BSE

E.1 Dirac structure of the pion BSE

The derivation of the dressing functions a_i begins by specifying the explicit momenta P^μ , p^μ and q^μ . In the pion's rest frame, the total pion momenta P^μ becomes:

$$P^\mu = iM \begin{pmatrix} 0 \\ 0 \\ 0 \\ 1 \end{pmatrix}^\mu. \quad (\text{E.1})$$

The total pion momentum is onshell, with $P^2 = -M^2$. This implies the existence of two independent Lorentz invariants: p^2 and z . Consequently, we can set $\phi = 0$ and $y = 1$. This immediately yields the result:

$$p^\mu = |p| \begin{pmatrix} 0 \\ 0 \\ \sqrt{1-z^2} \\ z \end{pmatrix}^\mu. \quad (\text{E.2})$$

It can be seen that the internal loop integration over q^μ includes a trivial integration over ϕ . Consequently, the choice of $\phi = 0$ allows the expression q^μ to be simplified to the form given in the equation.

$$q^\mu = |q| \begin{pmatrix} 0 \\ \sqrt{1-z'^2} \sqrt{1-y^2} \\ \sqrt{1-z'^2} y \\ z' \end{pmatrix}^\mu. \quad (\text{E.3})$$

Having specified the explicit momenta, we can write down the squared gluon momenta k^2 , as follows

$$k = p - q \implies k^2 = p^2 + q^2 - 2|p||q| \left(z z' + y \sqrt{1-z^2} \sqrt{1-z'^2} \right). \quad (\text{E.4})$$

The explicit input for the quark propagators, denoted by $S(p_\pm)$, then becomes

$$p_\pm = p \pm \frac{P}{2} \implies p_\pm^2 = p^2 + \frac{P^2}{4} \pm i M |p| z. \quad (\text{E.5})$$

The explicit vectors for our tensor basis in (4.11) become then

$$d^\mu = \begin{pmatrix} 0 \\ 0 \\ 0 \\ 1 \end{pmatrix}^\mu, \quad r^\mu = \begin{pmatrix} 0 \\ 0 \\ 1 \\ 0 \end{pmatrix}^\mu, \quad r'^\mu = \begin{pmatrix} 0 \\ \sqrt{1-y^2} \\ y \\ 0 \end{pmatrix}^\mu, \quad (\text{E.6})$$

where $r'^\mu = \hat{q}_\perp^\mu = q^\mu - \frac{q \cdot P}{P^2} P^\mu$ holds. Consequently, when contracted with the gamma matrices we arrive at the tensor basis $\tau_i \in \{\mathbb{1}, \not{d}, \not{r}, \not{r}'\not{d}\}$. Therefore, the vertex decomposition reads as

$$\Gamma(P; p) = \sum_{i=1}^4 a_i(p^2, z) \tau_i(r, d), \quad \tau_i \in \{\mathbb{1}, \gamma^4, \gamma^3, \gamma^3 \gamma^4\}. \quad (\text{E.7})$$

Respectively for the BSA inside the momentum loop, we have the following tensor basis:

$$\tau_i(r', d) \in \{\mathbb{1}, \gamma^4, \sqrt{1-y^2} \gamma^2 + y \gamma^3, \sqrt{1-y^2} \gamma^2 \gamma^4 + y \gamma^3 \gamma^4\}. \quad (\text{E.8})$$

It is convenient to define the pion Bethe-Salpeter wave function

$$\Psi(P; p) = S(p_+) \Gamma(P; p) S(p) = \Psi(P; p) \gamma^5. \quad (\text{E.9})$$

Since the Bethe-Salpeter wave function, $\Psi(P; p)$, has the same structural form as the vertex function, $\Gamma(P; p)$, it must have the same basis decomposition, as given in Equation E.7, except with different dressing functions, b_i .

$$\Psi(P; p) = \sum_{i=1}^4 b_i(p^2, z) \tau_i(P; p). \quad (\text{E.10})$$

In this manner, we introduced an intermediate step when solving the pion BSE

$$\Gamma(P; p) = \frac{16\pi}{3} Z_2^2 \int \frac{d^4 q}{(2\pi)^4} \frac{\alpha(k^2)}{k^2} T_k^{\mu\nu} \gamma^\mu \Psi(P; q) \gamma^\nu, \quad \Psi(P; p) = S(p_+) \Gamma(p, P) S(-p_-). \quad (\text{E.11})$$

The final step is to insert the vertex decompositions, as defined in Equations (E.7), (E.10), into (E.11) and multiply with $\bar{\tau}_i(r, d)$ from the left, in order to utilize the orthonormality relation for the basis. This will result in the following set of scalar equations for the dressing functions a_i and b_i :

$$a_i(p^2, z) = \frac{16\pi}{3} Z_2^2 \sum_{j=1}^4 \int \frac{d^4 q}{(2\pi)^4} \frac{\alpha(k^2)}{k^2} K_{ij}(p^2, q^2, z, z', y) b_j(q^2, z'), \quad (\text{E.12})$$

$$b_i(p^2, z) = \sum_{j=1}^4 G_{ij}(p^2, z) a_j(p^2, z).$$

The Dirac traces are embedded within the introduced matrices K_{ij} and G_{ij} as a means of providing a concise representation of their explicit expression as

$$K_{ij}(p^2, q^2, z, z', y) = \frac{1}{4} T_k^{\mu\nu} \text{tr}(\bar{\tau}_i(r, d) \gamma^\mu \tau_j(r', d) \gamma^\nu), \quad (\text{E.13})$$

$$G_{ij}(p^2, z) = \frac{1}{4} \text{tr}(\bar{\tau}_i(r, d) S(p_+) \tau_j(r, d) S(-p_-)).$$

Prior to presenting the explicit matrix elements of K_{ij} , it is advisable to adopt a simplified notation to enhance readability. Accordingly, K_{ij} can be expressed as $K_{ij} = \frac{1}{k^2} \tilde{K}_{ij}$ and the variables u , u' can be defined and introduced as follows: $u = p \sqrt{1 - z^2}$ and $u' = q \sqrt{1 - z'^2}$. This approach will enable a more concise and organized presentation of the subsequent results.

$$\begin{aligned}
\tilde{K}_{11} &= 3k^2, \\
\tilde{K}_{22} &= -2(pz - qz')^2 - k^2, \\
\tilde{K}_{23} &= -2(uy - u')(pz - qz') \\
\tilde{K}_{32} &= -2(u - u'y)(pz - qz'), \\
\tilde{K}_{33} &= 2uu'(1 + y^2) - 2y(u^2 + u'^2) - yk^2, \\
\tilde{K}_{44} &= yk^2 - 2uu'(1 - y^2),
\end{aligned} \tag{E.14}$$

The remaining matrix elements are zero.

Furthermore, the quark propagators $S(p_\pm^2)$ indicate that G_{ij} will contain a common factor, which is expressed by the relation

$$G_{ij} = \frac{1}{A(p_-^2)} \frac{1}{p_-^2 - M^2(p_-^2)} \frac{1}{A(p_+^2)} \frac{1}{p_+^2 - M^2(p_+^2)} \tilde{G}_{ij}. \tag{E.15}$$

This simplifies the notation, thereby allowing for a more concise representation of the underlying mathematical structure. In the following, the pion's four-momenta, $P^2 = -M^2$, will be written as $P^2 = -m_\pi^2$ with the aim of improving readability and avoiding confusion with the quark's mass function, $M(p_\pm^2)$.

$$\begin{aligned}
\tilde{G}_{11} &= \frac{m_\pi^2}{4} + M(p_-^2) M(p_+^2) + p^2, \\
\tilde{G}_{21} &= \frac{1}{2} (M(p_-^2) (m_\pi - 2ipz) + M(p_+^2) (m_\pi + 2ipz)), \\
\tilde{G}_{22} &= \frac{m_\pi^2}{4} + M(p_-^2) M(p_+^2) + p^2(2z^2 - 1), \\
\tilde{G}_{31} &= -ip \sqrt{1 - z^2} (M(p_-^2) - M(p_+^2)), \\
\tilde{G}_{32} &= 2p^2 z \sqrt{1 - z^2}, \\
\tilde{G}_{33} &= -\frac{m_\pi^2}{4} + M(p_-^2) M(p_+^2) - p^2(2z^2 - 1), \\
\tilde{G}_{41} &= -im_\pi p \sqrt{1 - z^2}, \\
\tilde{G}_{42} &= -ip \sqrt{1 - z^2} (M(p_-^2) + M(p_+^2)), \\
\tilde{G}_{43} &= \frac{1}{2} (M(p_+^2) (m_\pi + 2ipz) - M(p_-^2) (m_\pi - 2ipz)), \\
\tilde{G}_{44} &= -\frac{m_\pi^2}{4} + M(p_-^2) M(p_+^2) - p^2.
\end{aligned} \tag{E.16}$$

where the remaining elements are fixed by the property that G_{ij} is symmetric, which implies that $G_{ij} = G_{ji}$.

Appendix F

Further information to the quark-photon vertex

F.1 Dirac structure of the quark-photon vertex

In this context, the approach taken is analogous to that described in App. E.1 for the case of the pion BSE. This involves the specification of a specific frame, with the rest frame of the photon chosen as the reference frame

$$Q^\mu = |Q| \begin{pmatrix} 0 \\ 0 \\ 0 \\ 1 \end{pmatrix}^\mu, \quad k^\mu = |k| \begin{pmatrix} 0 \\ 0 \\ \sqrt{1-z^2} \\ z \end{pmatrix}^\mu, \quad k'^\mu = |k'| \begin{pmatrix} 0 \\ \sqrt{1-z'^2} \sqrt{1-y^2} \\ \sqrt{1-z'^2} y \\ z' \end{pmatrix}^\mu. \quad (\text{F.1})$$

Since the equations are fully Lorentz-invariant it is not necessary to specify any frame at any point: In the end, the equations break down to the Lorentz-invariant quantities Q^2 , k^2 , $k \cdot Q$, k'^2 , $k' \cdot Q$ and $k \cdot k'$. It is nevertheless useful to specify this frame because it makes calculations easier. Once the frame has been specified, it can be seen that the four-vectors from (5.9) become

$$n^\mu = \begin{pmatrix} 0 \\ 0 \\ 0 \\ 1 \end{pmatrix}^\mu, \quad m^\mu = \begin{pmatrix} 0 \\ 0 \\ 1 \\ 0 \end{pmatrix}^\mu, \quad m'^\mu = \begin{pmatrix} 0 \\ \sqrt{1-y^2} \\ y \\ 0 \end{pmatrix}^\mu, \quad (\text{F.2})$$

with $m'^\mu = k'^\mu - \frac{k' \cdot Q}{Q} Q^\mu$. The new orthonormal basis can then be constructed as

$$\begin{aligned} [\tau_1^{qp}]^\mu &= \frac{1}{\sqrt{2}} \gamma_\perp^\mu, & [\tau_5^{qp}]^\mu &= m^\mu \mathbb{1}, & [\tau_9^{qp}]^\mu &= n^\mu \mathbb{1}, \\ [\tau_2^{qp}]^\mu &= \frac{1}{\sqrt{2}} \gamma_\perp^\mu \not{n}, & [\tau_6^{qp}]^\mu &= m^\mu \not{n}, & [\tau_{10}^{qp}]^\mu &= n^\mu \not{n}, \\ [\tau_3^{qp}]^\mu &= \frac{1}{\sqrt{2}} \gamma_\perp^\mu \not{m}, & [\tau_7^{qp}]^\mu &= m^\mu \not{m}, & [\tau_{11}^{qp}]^\mu &= n^\mu \not{m}, \\ [\tau_4^{qp}]^\mu &= \frac{1}{\sqrt{2}} \gamma_\perp^\mu \not{m} \not{n}, & [\tau_8^{qp}]^\mu &= m^\mu \not{m} \not{n}, & [\tau_{12}^{qp}]^\mu &= n^\mu \not{m} \not{n}. \end{aligned} \quad (\text{F.3})$$

The new vertex decomposition reads then as

$$\Gamma_{qp}^\mu(k, Q) = \sum_{j=1}^{12} a_j^{qp}(k^2, z, Q^2) i [\tau_j^{qp}(m, n)]^\mu. \quad (\text{F.4})$$

Following the insertion of the RL truncated kernel, $K^{(4)}$, and the splitting of the BSE into a two-step process, analogous to the method employed in the pion BSE case, we find that

$$\begin{aligned} \Gamma_{qp}^\mu(k, Q) &= Z_2 i \gamma^\mu - \frac{16\pi}{3} Z_2^2 \int \frac{d^4 k'}{(2\pi)^4} \frac{\alpha(l^2)}{l^2} T_l^{\alpha\beta} \gamma^\alpha \Psi(k', Q) \gamma^\beta, \\ \Psi(k, Q) &= S(k_+) \Gamma_{qp}^\mu(k, Q) S(k_-) = \sum_{j=1}^{12} b_j^{qp}(k^2, z, Q^2) i [\tau_j^{qp}(m, n)]^\mu, \end{aligned} \quad (\text{F.5})$$

where $l = k - k'$ is the transferred momentum over the gluon and the quark momenta are $k_\pm = k \pm \frac{Q}{2}$. The newly defined basis is orthonormal, and thus the scalar coupled integral equations for the dressing functions a_j^{qp} and b_j^{qp} are projected out by multiplying (F.5) by $\bar{\tau}_i^{qp}$ from the left:

$$\begin{aligned} a_i^{qp}(k^2, z, Q^2) &= Z_2 \tilde{a}_i^{qp} - \frac{16\pi}{3} Z_2^2 \sum_{j=1}^{12} \int \frac{d^4 k'}{(2\pi)^4} \frac{\alpha(l^2)}{l^2} K_{ij}^{qp}(k^2, k'^2, z, z', y, Q^2) b_j^{qp}(k'^2, z', Q^2), \\ b_i^{qp}(k^2, z, Q^2) &= \sum_{j=1}^{12} G_{ij}^{qp}(k^2, z, Q^2) a_j^{qp}(k^2, z, Q^2). \end{aligned} \quad (\text{F.6})$$

The Dirac traces are embedded within the introduced matrices $K_{ij}^{qp}(k^2, k'^2, z, z', y, Q^2)$, $G_{ij}^{qp}(k^2, z, Q^2)$ and in the inhomogeneous term \tilde{a}_i^{qp}

$$\begin{aligned} K_{ij}^{qp}(k^2, k'^2, z, z', y, Q^2) &= \frac{1}{4} T_k^{\alpha\beta} \text{tr}([\bar{\tau}_i(m, n)]^\mu \gamma^\alpha [\tau_j(m', n)]^\mu \gamma^\beta), \\ G_{ij}^{qp}(k^2, z, Q^2) &= \frac{1}{4} \text{tr}([\bar{\tau}_i(m, n)]^\mu S(k_+) [\tau_j(m, n)]^\mu S(k_-)), \\ \tilde{a}_i^{qp} &= \frac{1}{4} \text{tr}([\bar{\tau}_i(m, n)]^\mu \gamma^\mu). \end{aligned} \quad (\text{F.7})$$

The explicit trace for \tilde{a}_i^{qp} is

$$\tilde{a}_i^{qp} = \begin{cases} \sqrt{2}, & i = 1 \\ 1, & i = 7, 10 \\ 0, & \text{else} \end{cases} \quad (\text{F.8})$$

Prior to presenting the explicit matrix elements of K_{ij}^{qp} , it is advisable to adopt a simplified notation to enhance readability. Accordingly, K_{ij}^{qp} can be expressed as $K_{ij}^{qp} = \frac{1}{l^2} \tilde{K}_{ij}^{qp}$ and the variables u, u' can be defined and introduced as follows: $u = k \sqrt{1 - z^2}$ and $u' = k' \sqrt{1 - z'^2}$. This approach will enable a more concise and organized presentation of the subsequent results:

$$\begin{aligned}
\tilde{K}_{11}^{qp} &= -\frac{1}{2} k^2 (y^2 + 1) + (2 y^3 u u' + k k' z z' (y^2 + 1)) - \frac{1}{2} k'^2 (y^2 + 1), \\
\tilde{K}_{16}^{qp} &= \sqrt{2} (y^2 - 1) u' (k' z' - k z), \\
\tilde{K}_{17}^{qp} &= \frac{1}{\sqrt{2}} (y^2 - 1) (k^2 - 2 (2 y u u' + k k' z z') + k'^2 (3 - 2 z'^2)), \\
\tilde{K}_{22}^{qp} &= \frac{1}{2} (k^2 (y^2 + 1) (2 z^2 - 1) - 2 k k' z z' (y^2 + 1) + k'^2 (y^2 + 1) (2 z'^2 - 1) + 4 u u' y), \\
\tilde{K}_{23}^{qp} &= ((2 u y - u' (y^2 + 1)) (k z - k' z')), \\
\tilde{K}_{28}^{qp} &= \tilde{K}_{71}^{qp} + \sqrt{2} (1 - y^2), \\
\tilde{K}_{32}^{qp} &= (u y^2 + u - 2 u' y) (k z - k' z'), \\
\tilde{K}_{33}^{qp} &= k^2 (y - 2 y z^2) - u u' (y^2 + 1) + 2 y k k' z z' + k'^2 y (1 - 2 z'^2), \\
\tilde{K}_{38}^{qp} &= -\tilde{K}_{61}^{qp}, \\
\tilde{K}_{44}^{qp} &= k^2 y + u u' (-3 y^2 + 1) - 2 y k k' z z' + k'^2 y, \\
\tilde{K}_{55}^{qp} &= 3 l^2 y, \\
\tilde{K}_{61}^{qp} &= \sqrt{2} u (y^2 - 1) (k z - k' z'), \\
\tilde{K}_{66}^{qp} &= -y (2 (k z - k' z')^2 + l^2), \\
\tilde{K}_{67}^{qp} &= 2 y (u' - u y) (k z - k' z'), \\
\tilde{K}_{71}^{qp} &= \frac{1}{\sqrt{2}} (y^2 - 1) (k'^2 - 2 (2 y u u' + k k' z z') + k^2 (3 - 2 z^2)), \\
\tilde{K}_{76}^{qp} &= 2 y (u' y - u) (k z - k' z'), \\
\tilde{K}_{77}^{qp} &= y (k^2 y (2 z^2 - 3) + 2 u u' (2 y^2 + 1) + 2 y k k' z z' + k'^2 y (2 z'^2 - 3)), \\
\tilde{K}_{82}^{qp} &= \tilde{K}_{17}^{qp} + \sqrt{2} (1 - y^2) \\
\tilde{K}_{83}^{qp} &= -\tilde{K}_{16}^{qp}, \\
\tilde{K}_{99}^{qp} &= \frac{1}{y} \tilde{K}_{55}^{qp}, \\
\tilde{K}_{10,10}^{qp} &= \frac{1}{y} \tilde{K}_{66}^{qp}, \\
\tilde{K}_{10,11}^{qp} &= \frac{1}{y} \tilde{K}_{67}^{qp}, \\
\tilde{K}_{11,10}^{qp} &= \frac{1}{y} \tilde{K}_{76}^{qp}, \\
\tilde{K}_{11,11}^{qp} &= \frac{1}{y} \tilde{K}_{77}^{qp}, \\
\tilde{K}_{12,12}^{qp} &= \frac{1}{y} \tilde{K}_{88}^{qp}.
\end{aligned}
\tag{F.9}$$

All other matrix elements, which are not listed explicitly are 0.

Furthermore, the quark propagators $S(k_\pm^2)$ indicate that G_{ij}^{qp} will contain a common

factor, which is expressed by the relation

$$G_{ij}^{qp} = \frac{1}{A(k_-^2)} \frac{1}{k_-^2 - M^2(k_-^2)} \frac{1}{A(k_+^2)} \frac{1}{k_+^2 - M^2(k_+^2)} \tilde{G}_{ij}^{qp}. \quad (\text{F.10})$$

This simplifies the notation, thereby allowing for a more concise representation of the underlying mathematical structure as:

$$\begin{aligned} \tilde{G}_{11}^{qp} &= k^2 + M(k_-^2) M(k_+^2) - \frac{Q^2}{4}, \\ \tilde{G}_{12}^{qp} &= \frac{i}{2} (M(k_-^2) (2kz + Q) + M(k_+^2) (Q - 2kz)), \\ \tilde{G}_{13}^{qp} &= iu (M(k_-^2) - M(k_+^2)), \\ \tilde{G}_{14}^{qp} &= -Qu, \\ \tilde{G}_{22}^{qp} &= k^2 (2z^2 - 1) + M(k_-^2) M(k_+^2) - \frac{Q^2}{4}, \\ \tilde{G}_{23}^{qp} &= 2kuz, \\ \tilde{G}_{24}^{qp} &= iu (M(k_-^2) + M(k_+^2)), \\ \tilde{G}_{33}^{qp} &= k^2 (1 - 2z^2) + M(k_-^2) M(k_+^2) + \frac{Q^2}{4}, \\ \tilde{G}_{34}^{qp} &= -\frac{i}{2} (M(k_-^2) (2kz + Q) - M(k_+^2) (Q - 2kz)), \\ \tilde{G}_{44}^{qp} &= -k^2 + M(k_-^2) M(k_+^2) + \frac{Q^2}{4}, \\ \tilde{G}_{55}^{qp} &= \tilde{G}_{99}^{qp} = \tilde{G}_{44}^{qp}, \\ \tilde{G}_{56}^{qp} &= \tilde{G}_{9,10}^{qp} = \tilde{G}_{34}^{qp}, \\ \tilde{G}_{66}^{qp} &= \tilde{G}_{10,10}^{qp} = \tilde{G}_{33}^{qp}, \\ \tilde{G}_{77}^{qp} &= \tilde{G}_{11,11}^{qp} = \tilde{G}_{22}^{qp}, \\ \tilde{G}_{78}^{qp} &= \tilde{G}_{11,12}^{qp} = \tilde{G}_{12}^{qp}, \\ \tilde{G}_{88}^{qp} &= \tilde{G}_{12,12}^{qp} = \tilde{G}_{11}^{qp}, \\ \tilde{G}_{57}^{qp} &= \tilde{G}_{9,11}^{qp} = -\tilde{G}_{24}^{qp}, \\ \tilde{G}_{58}^{qp} &= \tilde{G}_{9,12}^{qp} = -\tilde{G}_{14}^{qp}, \\ \tilde{G}_{67}^{qp} &= \tilde{G}_{10,11}^{qp} = -\tilde{G}_{23}^{qp}, \\ \tilde{G}_{68}^{qp} &= \tilde{G}_{10,12}^{qp} = -\tilde{G}_{13}^{qp}. \end{aligned} \quad (\text{F.11})$$

The remaining elements are fixed by the fact that the propagating matrix G_{ij} is symmetric, which means that $G_{ij} = G_{ji}$ holds.

Bibliography

- [1] R. Hofstadter, “The electron-scattering method and its application to the structure of nuclei and nucleons.” <https://www.nobelprize.org/uploads/2018/06/hofstadter-lecture.pdf>, 1961. [Online; accessed 10-June-2024].
- [2] H. W. Kendall, “DEEP INELASTIC SCATTERING: EXPERIMENTS ON THE PROTON AND THE OBSERVATION OF SCALING.” https://fwe.ifj.edu.pl/uploads/Seminaria/ep_nobel/1_kendall_lecture.pdf, 1990. [Online; accessed 10-June-2024].
- [3] P. Maris and P. C. Tandy, “The Quark-Photon Vertex and the Pion Charge Radius,” *Physical Review C*, vol. 61, p. 045202, Mar. 2000. arXiv:nucl-th/9910033.
- [4] A. S. M. López, H. Sanchis-Alepuz, and R. Alkofer, “Elucidating the effect of intermediate resonances in the quark interaction kernel on the time-like electromagnetic pion form factor,” *Physical Review D*, vol. 103, p. 116006, June 2021. arXiv:2102.12541 [hep-ph].
- [5] F. Gross, Klempt, *et al.*, “50 Years of Quantum Chromodynamics,” *The European Physical Journal C*, vol. 83, p. 1125, Dec. 2023. arXiv:2212.11107 [hep-ex, physics:hep-lat, physics:hep-ph, physics:hep-th].
- [6] “The existence of a neutron,” *Proceedings of the Royal Society of London. Series A, Containing Papers of a Mathematical and Physical Character*, vol. 136, pp. 692–708, June 1932.
- [7] J. W. Cronin, “The 1953 Cosmic Ray Conference at Bagnères de Bigorre: the Birth of Sub Atomic Physics,” *The European Physical Journal H*, vol. 36, pp. 183–201, Sept. 2011.
- [8] J. Goldstone, A. Salam, and S. Weinberg, “Broken Symmetries,” *Physical Review*, vol. 127, pp. 965–970, Aug. 1962. Publisher: American Physical Society.
- [9] S. Jain and S. R. Wadia, “The Science of Murray Gell-Mann,” Sept. 2019. arXiv:1909.07354 [hep-ph, physics:hep-th, physics:nlin, physics:physics].
- [10] M. Gell-Mann, “The Eightfold Way: A Theory of Strong Interaction Symmetry*,” in *The Eightfold Way*, CRC Press, 2000. Num Pages: 47.
- [11] I. Neutelings, “Meson & baryon multiplets,” Sept. 2023.
- [12] N. N. Bogolubov, B. V. Struminsky, and A. N. Tavkhelidze, “On composite models in the theory of elementary particles,” Jan. 1965.

- [13] M. Y. Han and Y. Nambu, “Three Triplet Model with Double SU(3) Symmetry,” *Phys. Rev.*, vol. 139, pp. B1006–B1010, 1965.
- [14] Y. Miyamoto, “Three Kinds of Triplet Model,” *Progress of Theoretical Physics Supplement*, vol. E65, pp. 187–192, Aug. 2013.
- [15] Y. Nambu, “A systematics of hadrons in subnuclear physics,” in *Preludes in theoretical physics* (H. Feshbach and L. C. P. Van Hove, eds.), pp. 133–142, Amsterdam: North-Holland, 1966.
- [16] G. t. Hooft, “When was Asymptotic Freedom discovered? or The Rehabilitation of Quantum Field Theory,” *Nuclear Physics B - Proceedings Supplements*, vol. 74, pp. 413–425, Mar. 1999. arXiv:hep-th/9808154.
- [17] H. Fritzsch, M. Gell-Mann, and H. Leutwyler, “Advantages of the Color Octet Gluon Picture,” *Phys. Lett. B*, vol. 47, pp. 365–368, 1973.
- [18] D. J. Gross and F. Wilczek, “Ultraviolet Behavior of Nonabelian Gauge Theories,” *Phys. Rev. Lett.*, vol. 30, pp. 1343–1346, 1973.
- [19] D. Gross and F. Wilczek, “A watershed: the emergence of QCD,” *quantum chromodynamics*, vol. 53, no. 1, 2013.
- [20] D. J. Gross, “Asymptotic Freedom and QCD—a Historical Perspective,” *Nuclear Physics B - Proceedings Supplements*, vol. 135, pp. 193–211, Oct. 2004.
- [21] G. Eichmann, “Hadron properties from QCD bound-state equations,” Sept. 2009. arXiv:0909.0703 [hep-lat, physics:hep-ph, physics:nucl-th].
- [22] G. Eichmann, H. Sanchis-Alepuz, R. Williams, R. Alkofer, and C. S. Fischer, “Baryons as relativistic three-quark bound states,” *Progress in Particle and Nuclear Physics*, vol. 91, pp. 1–100, Nov. 2016. arXiv:1606.09602 [hep-lat, physics:hep-ph, physics:nucl-th].
- [23] G. Eichmann, “QCD and Hadron Physics.”
- [24] R. Alkofer, “Computational Methods in Particle Physics.” 2021.
- [25] T. Banks, “Modern Quantum Field Theory: A Concise Introduction,”
- [26] G. Eichmann, “Euclidean conventions.” <http://cftp.ist.utl.pt/~gernot.eichmann/2020-QCDHP/App-Euclidean.pdf>, 2020. [Online; accessed 17-May-2024].
- [27] R. Mann, *An introduction to particle physics and the standard model*. Boca Raton, Fla.: CRC Press, 2010.
- [28] D. Bailin and A. Love, *Introduction to Gauge Field Theory*. New York: Routledge, 1 ed., Jan. 2019.
- [29] P. Maris and P. C. Tandy, “Bethe-Salpeter Study of Vector Meson Masses and Decay Constants,” *Physical Review C*, vol. 60, p. 055214, Oct. 1999. arXiv:nucl-th/9905056.
- [30] P. Maris and C. D. Roberts, “pi- and K-meson Bethe-Salpeter Amplitudes,” *Physical Review C*, vol. 56, pp. 3369–3383, Dec. 1997. arXiv:nucl-th/9708029.

- [31] R. Alkofer, P. Watson, and H. Weigel, “Mesons in a Poincare Covariant Bethe-Salpeter Approach,” *Physical Review D*, vol. 65, p. 094026, May 2002. arXiv:hep-ph/0202053.
- [32] A. Windisch, “The analytic properties of the quark propagator from an effective infrared interaction model,” *Physical Review C*, vol. 95, p. 045204, Apr. 2017. arXiv:1612.06002 [hep-ph, physics:nucl-th].
- [33] P. Maris, C. D. Roberts, and P. C. Tandy, “Pion mass and decay constant,” *Physics Letters B*, vol. 420, pp. 267–273, Feb. 1998. arXiv:nucl-th/9707003.
- [34] G. Eichmann, “4.5 Hadron matrix elements.” <http://cftp.ist.utl.pt/~gernot.eichmann/2020-QCDHP/QCD-hadron-matrix-elements.pdf>, 2020. [Online; accessed 30-May-2024].
- [35] A. S. Miramontes and H. Sanchis-Alepuz, “On the effect of resonances in the quark-photon vertex,” *The European Physical Journal A*, vol. 55, p. 170, Oct. 2019. arXiv:1906.06227 [hep-ph].
- [36] H. Sanchis-Alepuz and R. Williams, “Recent developments in bound-state calculations using the Dyson-Schwinger and Bethe-Salpeter equations,” *Computer Physics Communications*, vol. 232, pp. 1–21, Nov. 2018. arXiv:1710.04903 [hep-ph].
- [37] G. Eichmann, “Probing nucleons with photons at the quark level,” Apr. 2014. arXiv:1404.4149 [hep-ph, physics:nucl-th].
- [38] J. S. Ball and T.-W. Chiu, “Analytic properties of the vertex function in gauge theories. I,” *Physical Review D*, vol. 22, pp. 2542–2549, Nov. 1980. Publisher: American Physical Society.
- [39] I. S. M. Abramowitz, “Handbook of Mathematical Functions With Formulas, Graphs, and Mathematical Tables.” https://personal.math.ubc.ca/~cbm/aands/abramowitz_and_stegun.pdf, 1964. [Online; accessed 10-June-2024].
- [40] G. Eichmann, “QCD and Hadron Physics.” https://static.uni-graz.at/fileadmin/_Persoenliche_Webseite/eichmann_gernot/lecture-notes/QCDHP/Hadron-Physics.pdf, 2021. [Online; accessed 17-May-2024].
- [41] C. S. Fischer, “Infrared Properties of QCD from Dyson-Schwinger equations,” *Journal of Physics G: Nuclear and Particle Physics*, vol. 32, pp. R253–R291, Aug. 2006. arXiv:hep-ph/0605173.